ABC Cardiol
Arquivos Brasileiros de Cardiologia

Volume 116 | Number 2 | Supplement 1
February 2021

Brazilian Society of Cardiology
ISSN-0066-782X

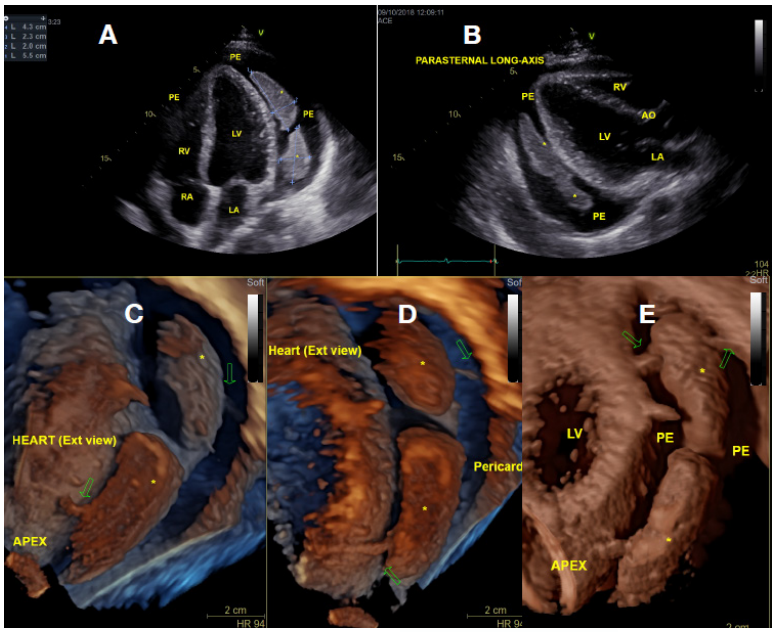

Figure 1 da Page 13

ABC Cardiol
Arquivos Brasileiros de Cardiologia
JOURNAL OF BRAZILIAN SOCIETY OF CARDIOLOGY - Published since 1943

Contents

ABC Cardiol
Arquivos Brasileiros de Cardiologia

JOURNAL OF BRAZILIAN SOCIETY OF CARDIOLOGY - Published since 1943

Sociedade Brasileira de Cardiologia

President
Marcelo Antônio Cartaxo Queiroga Lopes

Vice President
Celso Amodeo

Financial Director
Ricardo Mourilhe Rocha

Scientific Director
Fernando Bacal

Managing Director
Olga Ferreira de Souza

Service Quality Director
Sílvio Henrique Barberato

Communication Director
Harry Corrêa Filho

Information Technology Director
Leandro Ioschpe Zimerman

Governmental Relations Director
Nasser Sarkis Simão

State and Regional Relations Director
João David de Souza Neto

Cardiovascular Health Promotion Director – SBC/Funcor
José Francisco Kerr Saraiva

Director of Specialized Departments
Andréa Araujo Brandão

Research Director
David de Pádua Brasil

Coordinator of Science, Technology and Innovation
Ludhmila Abrahão Hajjar

Coordinator of Continued Medical Education
Brivaldo Markman Filho

Coordinator of Management Supervision and Internal Control
Gláucia Maria Moraes de Oliveira

Coordinator of Compliance and Transparency
Marcelo Matos Cascudo

Coordinator of Strategic Affairs
Hélio Roque Figueira

Editor-in-Chief of the Arquivos Brasileiros de Cardiologia
Carlos Eduardo Rochitte

Editor-in-Chief of the IJCS
Claudio Tinoco Mesquita

Coordinator of the University of the Heart
Evandro Tinoco Mesquita

Coordinator of Standards and Guidelines
Brivaldo Markman Filho

Presidents of State and Regional Brazilian Societies of Cardiology:
SBC/AL – Carlos Romerio Costa Ferro

SBC/AM – Kátia do Nascimento Couceiro

SBC/BA – Gilson Soares Feitosa Filho

SBC/CE – Gentil Barreira de Aguiar Filho

SBC/DF – Alexandra Oliveira de Mesquita

SBC/ES – Tatiane Mascarenhas Santiago Emerich

SBC/GO – Leonardo Sara da Silva

SBC/MA – Mauro José Mello Fonseca

SBC/MG – Henrique Patrus Mundim Pena

SBC/MS – Gabriel Doreto Rodrigues

SBC/MT – Marcos de Thadeu Tenuta Junior

SBC/NNE – Nivaldo Menezes Filgueiras Filho

SBC/PA – Dilma do Socorro Moraes de Souza

SBC/PB – Lenine Angelo Alves Silva

SBC/PE – Fernando Ribeiro de Moraes Neto

SBC/PI – Luiz Bezerra Neto

SBC/PR – Raul DAurea Mora Junior

SOCERJ – Wolney de Andrade Martins

SBC/RN – Maria Sanali Moura de Oliveira Paiva

SOCERON – Daniel Ferreira Mugrabi

SOCERGS – Mario Wiehe

SBC/SC – Amberson Vieira de Assis

SBC/SE – Eryca Vanessa Santos de Jesus

SOCESP – João Fernando Monteiro Ferreira

Presidents of the Specialized Departaments and Study Groups

SBC/DA – Antonio Carlos Palandri Chagas

SBC/DCC – Bruno Caramelli

SBC/DCC/CP – Klebia Magalhães Pereira Castello Branco

SBC/DCM – Celi Marques Santos

SBC/DECAGE – Izo Helber

SBC/DEIC – Evandro Tinoco Mesquita

SBC/DERC – Gabriel Leo Blacher Grossman

SBC/DFCVR – Antoinette Oliveira Blackman

SBC/DHA – Audes Diógenes de Magalhães Feitosa

SBC/DIC – Carlos Eduardo Rochitte

SBCCV – Eduardo Augusto Victor Rocha

SOBRAC – Ricardo Alkmim Teixeira

SBHCI – Ricardo Alves da Costa

DCC/GAPO – Danielle Menosi Gualandro

DCC/GECETI – Luiz Bezerra Neto

DCC/GECO – Roberto Kalil Filho

DCC/GEMCA – Roberto Esporcatte

DCC/GERTC – Adriano Camargo de Castro Carneiro

DEIC/GEICPED – Estela Azeka

DEIC/GEMIC – Marcus Vinicius Simões

DERC/GECESP – Clea Simone Sabino de Souza Colombo

DERC/GECN – Lara Cristiane Terra Ferreira Carreira

DERC/GERCPM – Carlos Alberto Cordeiro Hossri

GECIP – Marcelo Luiz da Silva Bandeira

GEECG – Carlos Alberto Pastore

DCC/GETA – Carlos Vicente Serrano Junior

DCC/GECRA – Sandra Marques e Silva

Arquivos Brasileiros de Cardiologia

Volume 116, Nº 2, Suppl. 1, February 2021

Indexing: ISI (Thomson Scientific), Cumulated Index Medicus (NLM), SCOPUS, MEDLINE, EMBASE, LILACS, SciELO, PubMed

Address: Av. Marechal Câmara, 160 - 3º andar - Sala 330
20020-907 • Centro • Rio de Janeiro, RJ • Brasil
Phone.: (21) 3478-2700
E-mail: arquivos@cardiol.br
http://abccardiol.org/
SciELO: www.scielo.br

Commercial Department
Phone: (11) 3411-5500
E-mail: comercialsp@cardiol.br

Editorial Production
SBC - Internal Publication Department

Graphic Design and Diagramming
SBC - Internal Design Department

Case Report

Covid-19 in Heart Transplant Recipients in São Paulo: A Case Series

Rafaela Vale de Miranda Soriano,[1] João Manoel Rossi Neto,[1] Marco A. Finger,[1] Carolina Casadei Santos[1]

Instituto Dante Pazzanese de Cardiologia,[1] São Paulo, SP - Brazil

Introduction

The disease caused by the new coronavirus (Covid-19), SARS-CoV-2 (severe acute respiratory syndrome coronavirus 2), was declared a pandemic by the World Health Organization (WHO) on March 11, 2020.[1] By analogy to others respiratory infections, mainly based on the 2009 pandemic of the influenza virus H1N1,[2,3] an increase in cases of pneumonia and progression to septic shock with acute respiratory distress syndrome was expected among recipients of solid-organ transplantation with Covid-19 in comparison with the non-transplanted population.[4] However, immunosuppression in transplantation could theoretically revoke the hyperinflammatory syndrome secondary to the cytokine storm, responsible for the majority of deaths by Covid-19.[5,6] Data on immunosuppression potentially leading to atypical clinical presentations or increasing the risk of adverse events in the presence of Covid-19 are conflicting.[7,8]

We report our experience with heart transplant (HT) recipients diagnosed with Covid-19 at an institution with an HT program since 1992 in São Paulo, Brazil.

Material and Methods

Population and Scenario

Adult HT recipients seen at the Dante Pazzanese cardiology institute between March and June 2020, with signs and symptoms suggestive of SARS-CoV-2 infection and who tested positive for polymerase chain reaction with reverse transcriptase (RT-PCR), or with radiological findings compatible with Covid-19.

Data were collected from medical records. Clinical history, laboratory results, inflammatory and radiological markers, and therapies administered were included. We describe death by Covid-19, admission to the Intensive Care Unit (ICU), need for mechanical ventilation, and renal dysfunction.

Keywords

Cardiovascular Diseases/surgery; Heart Transplantation: Coronavirus, Betacoronavirus; Covid-19; Severe Acute Respiratory Syndrome; SARS-CoV2; Transplant Recipients; Inflammation.

Mailing Address: Rafaela Vale de Miranda Vale de Miranda Soriano • Instituto Dante Pazzanese de Cardiologia - Transplante de Coração – Av. Dante Pazzanese, 500. Postal Code 04012-909, Ambulatório de Transplante de Coração, São Paulo, SP – Brazil
E-mail: rafavaledemiranda@yahoo.com.br
Manuscript received July 03, 2020, revised manuscript August 18, 2020, accepted Sepember 09, 2020

DOI: https://doi.org/10.36660/abc.20200722

Statistical Methods

Results are reported in a descriptive manner.

Results

Five HT patients were hospitalized due to Covid-19. None of them were diagnosed by asymptomatic screening.

The age ranged from 35 to 79 years. Comorbidities were diabetes mellitus (DM) (100%), systemic arterial hypertension (SAH) (80%), chronic kidney disease (40%) and obesity (20%). HT time ranged from 3 to 264 months. Calcineurin inhibitors were administered to four patients (80%), mTOR inhibitor to 40% of them, and prednisone and mycophenolate to 100%. The symptoms were documented fever (80%), cough on admission (100%), dyspnea (60%), and gastrointestinal symptoms (20%) (Table 1).

According to Table 2, lymphopenia (<1,500 mm^3) occurred in all patients and thrombocytopenia (<150,000 mm^3) in 60% of them. Troponin was elevated in one case of death, while in the other it was not assessed. There was also a change in lactate in a patient who died. Increased inflammatory markers were common, being higher in those who required intensive care. Chest computed tomography (CT) scan was performed in all patients, who had bilateral pulmonary infiltrates with a ground-glass appearance. Renal failure was present in 80% of the sample.

As described in Table 3, two patients did not receive empirical therapies for Covid-19. Vasopressors and mechanical ventilation were required in 20% of patients. None of them received extracorporeal membrane oxygenation. No patient was put in prone position and the length of stays at the ICU was four days for both patients who needed this care.

Immunosuppressants were discontinued in one patient due to the severity of the case. Two patients died (40%), and the rest were discharged from hospital. The length of stay varied between 4 and 21 days.

Discussion

This is the first description of a case series of a cohort of HT patients who were hospitalized by Covid-19 in Brazil.

These patients appear to present Covid19 similarly to non-transplanted patients, sharing the most common symptoms of fever, cough, and shortness of breath. In contrast to the study by Scott,[9] gastrointestinal symptoms were observed in only one patient (20%).

All HT recipients that were affected by Covid-19 required hospitalization, with DM being present in 100% of them and SAH in 80%. In our sample, 40% of patients required intensive care and had D-Dimer ≥1000 mg/L and CRP

Table 1 – Epidemiological data and symptoms associated with SARS-CoV-2 infection in HT recipients

Patients	Age (years)	Sex	Time of transplantation (meses)	Comorbidities	Immunosuppression	Symptoms
1	79	Male	264	SAH, DM, CKD	CI, AM, CE	Fever, cough, dyspnea
2	67	Male	264	SAH, DM, CKD	imTOR, AM, CE	Cough, dyspnea
3	52	Female	192	SAH, DM, Obesity	CI, AM	Fever, cough, dyspnea
4	50	Male	84	SAH DM	CI, imTOR, AM, CE	Fever, cough, GIS
5	35	Female	3	DM	CI, AM, CE	Fever, cough

SAH: systemic arterial hypertension; DM: diabetes mellitus; CKD: chronic kidney disease; CI: calcineurin inhibitor; imTOR: mTOR inhibitor; AM: antimetabolic; CE: corticosteroid; GIS: gastrointestinal symptoms.

Table 2 – Laboratory data associated with infection by SARS-CoV-2 in HT recipients

Patient	Total leucocytes (mm^3)	Total lymphocytes (mm^3)	Platelets <150000/mm^3	ARF	Trop I (ng/ml)	Dim-D (mg/L)	Lactate >2mmol	CRP	LDH	BNP
1	6,100	670	Yes	Yes	NC	1,836	No	20	397	NC
2	12,570	570	Yes	Yes	0.41	1,397	Yes	40	348	7,441
3	3,760	960	No	No	0.02	287	No	7.1	339	1,230
4	7,760	1,300	Yes	Yes	0.01	NC	No	0.5	NC	NC
5	8,350	420	No	Yes	0.03	675	No	1.1	NC	2,800

ARF: acute renal failure; Trop: troponin; Dim: dimer; CRP: C-reactive protein; LDH: lactic dehydrogenase; BNP: B-type natriuretic peptide; NC: not collected.

Table 3 – Diagnosis, therapy and outcomes associated with infection by SARS-CoV-2 in HT recipients

Patients	Diagnosis	Chest CT	Death	Length of hospital stay (days)	ICU	VAD	MV	Therapeutics
1	RT-PCR	<50%	Yes	4	Yes	No	No	Azithromycin
2	RT-PCR	>50%	Yes	4	Yes	Yes	Yes	HCQ, Azithromycin, CE
3	RT-PCR	<50%	No	11	No	No	No	NP
4	Chest CT	<50%	No	5	No	No	No	Azithromycin
5	RT-PCR	<50%	No	21	No	No	No	NP

RT-PCR: polymerase chain reaction for SARS-CoV-2; ICU: Intensive Care Unit; VAD: vasoactive drug; MV: mechanical ventilation; HCQ: hydroxychloroquine; CE: corticosteroid; NP: not performed; CT: computed tomography.

≥20. BNP was high and DHL did not show any significant increase when measured. The patient with elevated troponin presented hemodynamic instability, need for vasopressors and evolution to death, which corroborates the literature that associates myocardial injury with worse prognosis.[10] The patients who went to the ICU were elderly, with a longer heart transplantation period, and died. These data suggest a transplant mortality rate above that of the general population infected by Covid-19.[11]

The rates of lymphopenia and thrombocytopenia were higher in this study when compared with previous reports in the non-transplanted and transplanted populations.[12,13] This finding could be explained by a lower basal lymphocyte and platelet count due to the use of immunosuppressants or represent a likely additional interference from SARS-CoV-2 infection.

Our study has several limitations common to HT studies: the fact that it was performed in a single center and the size of our sample, which could be considered small. It was not possible to draw conclusions about specific treatments for Covid-19 or the management of immunosuppression in this scenario. This limits our understanding of the spectrum of symptoms and the severity of the disease among HT patients with Covid-19.

Conclusion

In this case series of HT patients with Covid-19 treated at our institution, the theoretical possibility that immunosuppression could revoke the hyperinflammatory syndrome was not proven true. From an observational point of view, the large number of risk factors and the high mortality rate suggest that these receptors could be particularly vulnerable to Covid-19. Further larger, multicenter studies are needed to confirm our findings.

Author contributions

Conception and design of the research: Soriano RVM, Rossi Neto JM, Santos CC; Acquisition of data: Soriano RVM; Analysis and interpretation of the data and Critical revision of the manuscript for intellectual content: Rossi Neto JM, Finger MA, Santos CC; Statistical analysis: Rossi Neto JM; Writing of the manuscript: Soriano RVM, Rossi Neto JM.

Potential Conflict of Interest

No potential conflict of interest relevant to this article was reported.

Sources of Funding

There were no external funding sources for this study.

Study Association

This study is not associated with any thesis or dissertation work.

Ethics approval and consent to participate

This article does not contain any studies with human participants or animals performed by any of the authors.

References

1. Zhu N, Zhang D, Wang W, Li X, Yang B, Song J, et al. A Novel Coronavirus from Patients with Pneumonia in China, 2019. N Engl J Med. 2020 20;382(8):727–33.
2. Cordero E, Pérez-Romero P, Moreno A, Len O, Montejo M, Vidal E, et al. Pandemic influenza A(H1N1) virus infection in solid organ transplant recipients: impact of viral and non-viral co-infection. Clin Microbiol Infect Off Publ Eur Soc Clin Microbiol Infect Dis. 2012 Jan;18(1):67–73.
3. Fernández-Ruiz M, Andrés A, Loinaz C, Delgado JF, López-Medrano F, San Juan R, et al. COVID-19 in solid organ transplant recipients: A single-center case series from Spain. Am J Transplant Off J Am Soc Transplant Am Soc Transpl Surg. 2020;20(7):1849–58.
4. Zhu L, Gong N, Liu B, Lu X, Chen D, Chen S, et al. Coronavirus Disease 2019 Pneumonia in Immunosuppressed Renal Transplant Recipients: A Summary of 10 Confirmed Cases in Wuhan, China. Eur Urol. 2020;77(6):748–54.
5. Mehta P, McAuley DF, Brown M, Sanchez E, Tattersall RS, Manson JJ, et al. COVID-19: consider cytokine storm syndromes and immunosuppression. Lancet Lond Engl. 2020 28;395(10229):1033–4.
6. Kumar D, Manuel O, Natori Y, Egawa H, Grossi P, Han S, et al. COVID-19: A global transplant perspective on successfully navigating a pandemic. Am J Transplant .2020;20(7):1773-9.'
7. Zhang H, Dai H, Xie X. Solid Organ Transplantation During the COVID-19 Pandemic. Front Immunol .2020;11:1392.
8. Yi SG, Rogers AW, Saharia A, Aoun M, Faour R, Abdelrahim M, et al. Early Experience With COVID-19 and Solid Organ Transplantation at a US High-volume Transplant Center. Transplantation.2020;104(11):2208-14..
9. Ketcham SW, Adie SK, Malliett A, Abdul-Aziz AA, Bitar A, Grafton G, et al. Coronavirus Disease-2019 in Heart Transplant Recipients in Southeastern Michigan: A Case Series. J Card Fail. 2020 .26(6):457-61.
10. Shi S, Qin M, Shen B, Cai Y, Liu T, Yang F, et al. Association of Cardiac Injury With Mortality in Hospitalized Patients With COVID-19 in Wuhan, China. JAMA Cardiol. 2020 5(7):802-10.
11. Wilson N, Kvalsvig A, Barnard LT, Baker MG. Case-Fatality Risk Estimates for COVID-19 Calculated by Using a Lag Time for Fatality. Emerg Infect Dis. 2020 Jun;26(6):1339–441.
12. Huang D, Lian X, Song F, Ma H, Lian Z, Liang Y, et al. Clinical features of severe patients infected with 2019 novel coronavirus: a systematic review and meta-analysis. Ann Transl Med. 2020 May;8(9):576.
13. Akalin E, Azzi Y, Bartash R, Seethamraju H, Parides M, Hemmige V, et al. Covid-19 and Kidney Transplantation. N Engl J Med. 2020 18;382(25):2475–7.

Antenatal Diagnosis of Double Aortic Arch

Natália Noronha,[1] *Angie Hobbs,*[1] *Patricia Caldas*[1]

Bristol Royal Hospital for Children,[1] *Bristol - United Kingdom*

Introduction

Congenital anomalies of the aortic arch affect 1-2% of the population and comprise a wide variety of abnormalities in the position and/or branching pattern of the aortic arch.[1] Double aortic arch (DAA) represents 1-2% of all aortic arch anomalies and is characterized by persistence of both left and right embryonic aortic arches.[2] It can be found either in isolation or, less frequently, in association with other cardiovascular or chromosomal abnormalities. Antenatal diagnosis of DAA may be challenging, as its distinction from other arch abnormalities like right aortic arch with left arterial duct or with an aberrant left subclavian artery is not always straightforward. The authors describe a case of antenatal diagnosis of DAA.

Case Report

A 26-year-old primigravida was referred for a fetal cardiology review at 23+3 weeks of gestation due to an abnormal three vessels and trachea (3VT) view in her routine 20-week anomaly scan. She was on no medications and there was no relevant personal or family history.

The fetal echocardiogram showed normal four-chamber view and outflow tracts. In the 3VT view, however, the arterial duct was seen on the left side of the trachea and the aortic arch was on the right side, confirming the presence of a right aortic arch with a left sided arterial duct (Figure 1). On a closer look, a smaller structure was seen on the left side of the trachea, completely encircling the latter. To confirm the diagnosis of DAA, the subclavian arteries were located and each one was seen to arise from the respective aortic arch (Figure 2). There were no signs of obstruction in either aortic arch. No other cardiac or extracardiac abnormalities were found. Given the possible association of DAA with chromosomal abnormalities, particularly the 22q11.2 microdeletion, the couple was advised to undergo invasive testing, which they declined.

After the delivery, a postnatal scan confirmed the antenatal findings (Figure 3). At 2 months of age, his parents noticed mild intermittent stridor. The patient was referred for a cardiac computerized tomography, which confirmed the diagnosis of a double aortic arch with atresia of the distal left arch (Figure 4). The patient underwent surgical division of the left arch at 3 months of age, which was complicated by left vocal cord palsy.

The patient is currently 5-months-old, has intermittent stridor due to bronchomalacia and left vocal cord palsy, and is fed by a nasogastric tube.

Discussion

DAA is the most frequent substrate for a vascular ring and might result in respiratory and/or digestive symptoms from an early age. In the majority of cases, one of the arches is dominant, more frequently the right arch (at least 75% of cases).[2] There may be an atretic segment in one or several locations in either arch, usually the left,[1,3] as happened in our case. DAA results in respiratory symptoms like stridor, choking episodes and recurrent respiratory tract infections in 91% of patients. Gastrointestinal symptoms, on the other hand, occur in 40% of cases and include vomiting, feeding intolerance in infants and dysphagia in older children and adults.[2,4]

The diagnosis of DAA can be made in the 3VT view described by Yagel et al.[5] In this view, the normal (left) aortic arch is observed on the left of the midline and the trachea. The arterial duct is seen laterally on its left side. The aortic arch and arterial duct then converge into a V-shaped structure that continues as the descending aorta. The third vessel that comprises the 3VT view is the *superior vena cava*, which is seen on the right of the midline. In a normal left aortic arch, no major vascular structures are seen to cross the trachea posteriorly. Conversely, in DAA the 3VT view depicts both a left and a right aortic arch, forming a vascular ring that completely encircles the trachea. This ring, together with the arterial duct, forms the figure of either a "6" or a "9" (also described as a trident shape) instead of the classic V-shaped structure described above. The presence of antegrade flow in both arches and in the arterial duct can be confirmed by color flow mapping. The latter should also be used to confirm or exclude obstruction to flow in any of the arches.

It may be difficult to distinguish DAA from other aortic arch abnormalities, such as right aortic arch with left arterial duct in the 3VT view. In this situation, the identification of the origin of the subclavian arteries may aid in the differential diagnosis. If each of the subclavian arteries is seen to arise from the left and right aortic arches (to the left and to the right side of the trachea, respectively), the diagnosis of DAA can be established.

Early surgical repair of DAA has been reported to eliminate symptoms in over 70% of cases, although airflow limitation might persist due to residual tracheal stenosis.[2] In a review of 183 patients with vascular rings who underwent surgical repair,[6] 2 patients required tracheostomy due to severe distal tracheal compression and one patient had true left vocal cord palsy, as happened with our case.

Keywords

Heart Defects Congenital/diagnosis; Heart Defects Congenital/surgery; Aorta Thoracic; Chromosome Aberrations; Ultrasonography/methods; Echocardiography/methods; Vocal Cord, Paralysis; Bronchomalacia/congenital.

Mailing Address: Natália Noronha •
Fetal Cardiology Service, Bristol Royal Hospital for Children, Bristol, United Kingdom - Upper Maudlin St Bristol BS2 8BJ - United Kingdom
E-mail: natalianoronhaf@gmail.com
Manuscript received May 11, 2019, revised mnauscript September 01, 2020, accepted November 26, 2019

DOI: https://doi.org/10.36660/abc.20190310

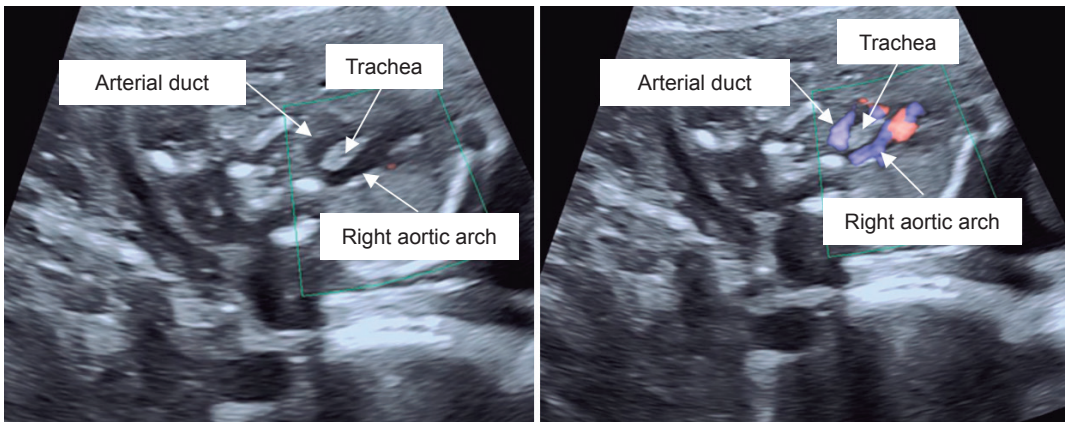

Figure 1 – *Fetal echocardiogram (three vessels and trachea view) showing a left arterial duct and a right aortic arch completely encircling the trachea without (left panel) and with (right panel) color flow mapping.*

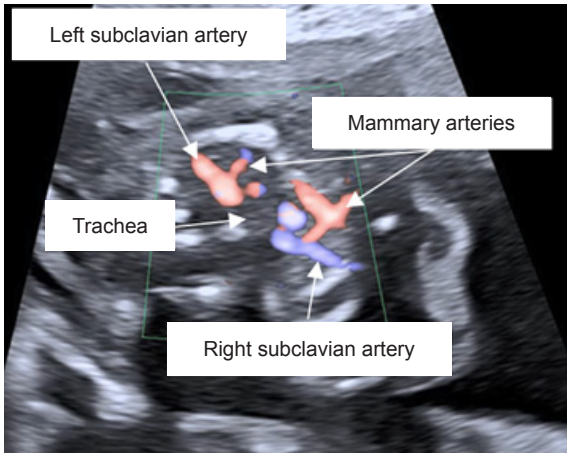

Figure 2 – *Fetal echocardiogram (color flow axial image) showing the left and the right subclavian arteries arising from the left and the right aortic arches, respectively.*

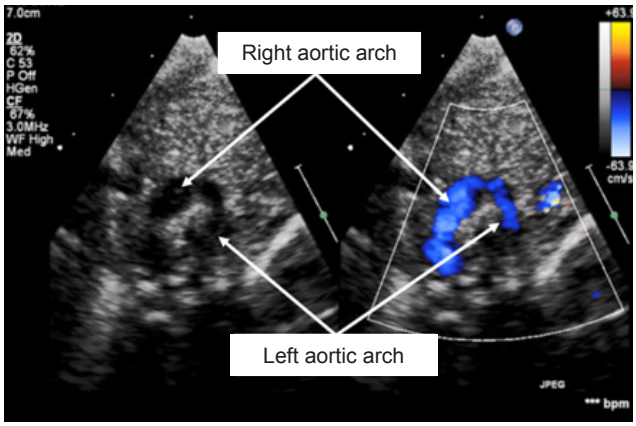

Figure 3 – *ETransthoracic echocardiogram - high parasternal view (2D and color flow mapping) showing the dominant right and the smaller left aortic arch.*

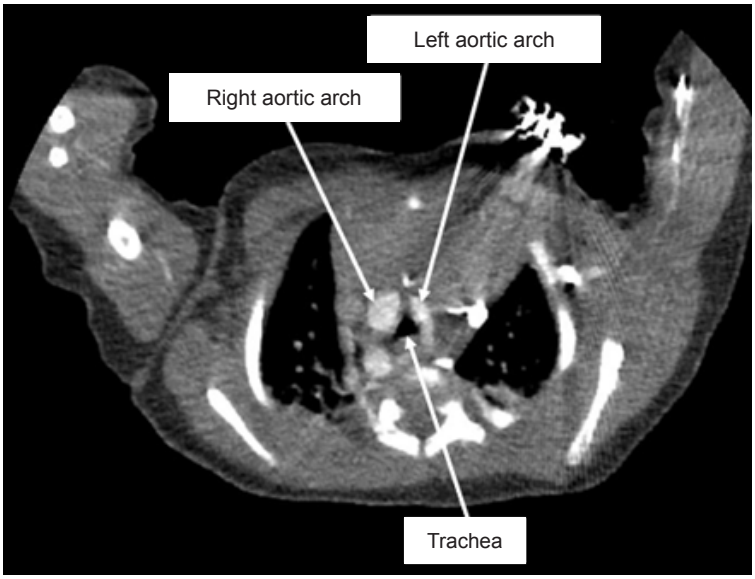

Figure 4 – *Computerized tomography scan - axial image showing the dominant right and the smaller left aortic arch.*

Albeit challenging, antenatal diagnosis of DAA enables a timely characterization of the vascular ring and facilitates planning of surgical intervention before or shortly after symptoms develop. Although symptoms may not be relieved immediately, an early division of the DAA is crucial to prevent long-term sequelae of tracheobronchial compression and feeding difficulties.[2]

Author Contributions

Acquisition of data: Hobbs A; Writing of the manuscript: Noronha N; Critical revision of the manuscript for intellectual content: Caldas P.

Potential Conflict of Interest

No potential conflict of interest relevant to this article was reported.

Sources of Funding

There were no external funding sources for this study.

Study Association

This study is not associated with any thesis or dissertation work.

Ethics approval and consent to participate

This article does not contain any studies with human participants or animals performed by any of the authors.

References

1. Trobo D, Bravo C, Alvarez T, Pérez R, Gámez F, León-Luis J. Prenatal Sonographic Features of a Double Aortic Arch: Literature Review and Perinatal Management. J Ultrasound Med. 2015;34(11):1921-7.
2. Gou Z, He Y, Zhang Y, Gu X. Prenatal diagnosis of fetal double aortic arch: report of a case. Int J Clin Exp Pathol. 2015;8(10):13565-7.
3. Schlesinger AE, Krishnamurthy R, Sena LM et al. Incomplete double aortic arch with atresia of the distal left arch: distinctive imaging appearance. AJR Am J Roentgenol. 2005;184(5):1634-9.
4. Krishnasarma R, Green Golan Mackintosh L, Bynum. ALTE and Feeding Intolerance as a Presentation of Double Aortic Arch. Case Rep Pediatr. 2016; 2016(5):1-3.
5. Yagel S, Arbel R, Anteby EY, Raveh D, Achiron R. The three vessels and trachea view (3VT) in fetal cardiac scanning. Ultrasound Obstet Gynecol. 2002 Oct;20(4):340-5.
6. Ruzmetov M, Vijay P, Rodefeld MD, Turrentine MW, Brown JW. Follow-up of surgical correction of aortic arch anomalies causing tracheoesophageal compression: a 38-year single institution experience. J Pediatr Surg. 2009;44(7):1328-32.

Coronary Vasoreactivity after Complete Bioresorption of Absorb BVS at 5-Year Follow-Up

Luis Renier Goncalves-Ramírez,[1] Hipólito Gutíerrez,[2] Fabián Julca,[2] Maximiliano Germán Amado Escañuela,[3] Gretel Varvaro,[4] Ignacio Amat-Santos[2]

Hospital de León – Cardiologia,[1] León - Spain
Hospital Clinico Universitario de Valladolid,[2] Castilla y León - Spain
Hospital General de Segovia,[3] Castilla y León - Spain
Hospital General de Palencia Río Carrión,[4] Castilla y León - Spain

Introduction

Bioresorbable coronary scaffolds have been designed to prevent long-term complications related to permanent implantation of metallic stents. Everolimus-eluting bioresorbable vascular scaffold (Absorb BVS; Abbott Vascular, Santa Clara, California) was one of the first bioresorbable vascular scaffolds (BVS) to be developed. Absorb BVS is a backbone of Poly-L-lactic acid coated with Poly-DL-lactic polymer, which elutes antiproliferative drug everolimus.[1] BVS received CE Mark for the treatment of coronary artery disease in January 2011 and it was marketed in most European countries by 2012.[2] Although good outcomes were initially described,[3,4] recent studies have questioned the safety of the device, suggesting a higher incidence of thrombosis and myocardial infarction.[5,6] Beyond this, structural and functional recovery of scaffolded coronary segments after BVS resorption has not been systematically searched in a consecutive real-world series.[7] We describe a case of a patient who was studied by coronary angiography, optical coherence tomography (OCT) and coronary vasoreactivity test 5-year after BVS implantation.

Case Report

A 39-year-old man, ex-smoker, presented with atypical chest pain and non-conclusive ischemia test. Past history included a ST-segment elevation myocardial infarction (STEMI) 5 years ago, in relation to a single-vessel disease treated with a 3.5x28mm Absorb BVS into mid left anterior descending (LAD). Now, the patient underwent a new coronary catheterization and there was no evidence of new lesions or restenosis. Then, an optical coherence tomography (OCT) was performed over the scaffolded segment of LAD showing fully reabsorbed Absorb BVS with development of a well-organized neointimal layer (Figure 1, Video1).

Keywords

Absorbable Implants/standards; Percutaneous Coronary Intervention/methods; Tissue Scaffolds/standards; Coronary Artery Disease; Myocardial Infarction;Recovery of Function.

Mailing Address: Luis Renier Goncalves-Ramírez •
Hospital de León – Cardiologia - Altos de Navas León León 24071 – Spain
E-mail: luisrenier@hotmail.com
Manuscript received November 07, 2019, revised manuscript January 22, 2020, accepted January 22, 2020.

DOI: https://doi.org/10.36660/abc.20190783

Coronary vasoreactivity was assessed with administration of intracoronary acetylcholine. Incremental bolus of acetylcholine were infused (2μg-20μg-100μg) for 3 minutes each followed by electrocardiographic, hemodynamic, angiographic and OCT evaluation of the functional response. At peak dose of acetylcholine the patient developed chest pain and LAD spasm -including the scaffolded segment- as observed by both, angiography and OCT Figure 2, Video 2. Finally, an intracoronary bolus (200μg) of nitroglycerin was administered in order to relieve coronary spasm and symptoms. Repeated angiography and OCT confirmed the vasodilator response.

Discussion

BVS technologies are currently in the spotlight worldwide due to a higher than expected rate of long-term adverse events and growing questions regarding the full resorption of the device.[8] Moreover, evidence-based data of long-term functional outcomes of the vessels treated with BVS are still scarce.[9] Indeed, whether *in vivo* normal vasomotion is recovered or not remains unanswered.

To the best of our knowledge, this is the first case that shows both morphological and functional recovery of scaffolded coronary segments after 5-year of Absorb BVS implantation in a real-life patent. As it has been previously described, Absorb BVS is finally reabsorbed by the vessel 5-year after implantation, with a development of a signal-rich layer seen by OCT into the scaffolded segment, which corresponds to neointima and underlying tissue.[9,10] On the other hand, paradoxical vasoconstriction induced by acetylcholine and corrected by nitroglycerin adds unique information regarding functional recovery of scaffolded coronary arteries, suggesting that the endothelial from the neointima is sensitive to chemical stimuli but might present paradoxical response in certain cases.

Conclusion

Fully resorption of Absorb BVS was found at 5-year follow-up. After scaffold resorption, there seems to be an adequate healing process of the vascular endothelium with restoration of the morphological and functional properties.

Author Contributions

Conception and design of the research: Ramirez LRG, Gutíerrez H, Amat-Santos I; Acquisition of data: Ramirez LRG, Gutíerrez H, Julca F, Amado M, Varvaro G; Analysis and interpretation of the data: Ramirez LRG, Julca F, Amado M; Writing of the manuscript: Ramirez LRG; Critical revision of

the manuscript for intellectual content: Gutíerrez H, Varvaro G, Amat-Santos I.

Potential Conflict of Interest

No potential conflict of interest relevant to this article was reported.

Sources of Funding

There were no external funding sources for this study.

Study Association

This study is not associated with any thesis or dissertation work.

Ethics Approval and Consent to Participate

This study was approved by the Ethics Committee of the Hospital Clinico Universitario de Valladolid under the protocol number PI 18-994. All the procedures in this study were in accordance with the 1975 Helsinki Declaration, updated in 2013. Informed consent was obtained from all participants included in the study.

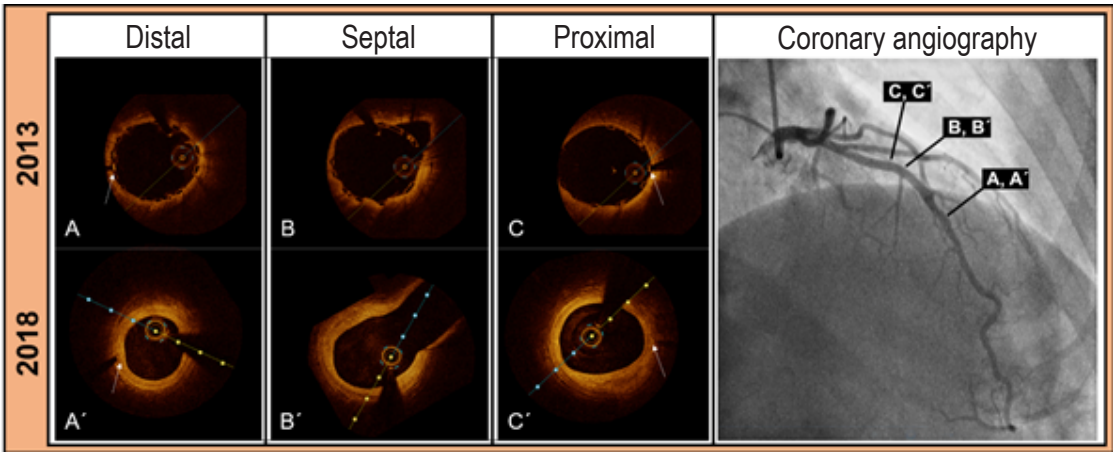

Figure 1 – *(A, B, C) Absorb-BVS implantation time-point by OCT. (A´, B´, C´) OCT findings at 5-year follow-up (same cross-section). White arrows point radiopaque markers of scaffolds.*

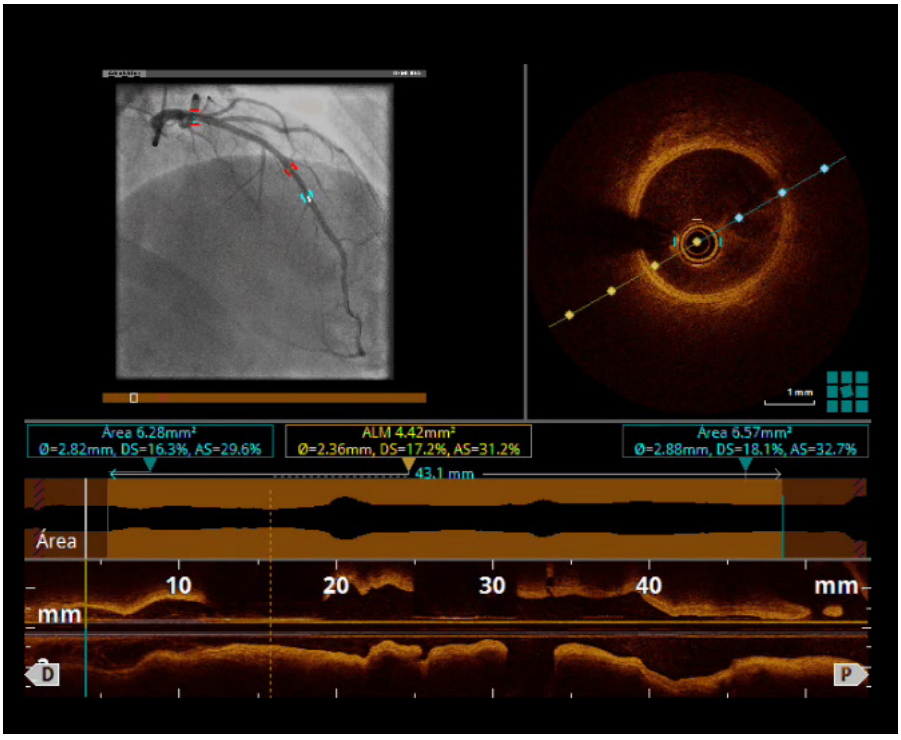

Video 1 – *Optical coherence tomography performed over the scaffolded segment of LAD showing fully reabsorbed Absorb BVS and a well-organized neointimal layer. Access the video at the link: http://abccardiol.org/supplementary-material/2021/11601/2019-0783-video1.mp4*

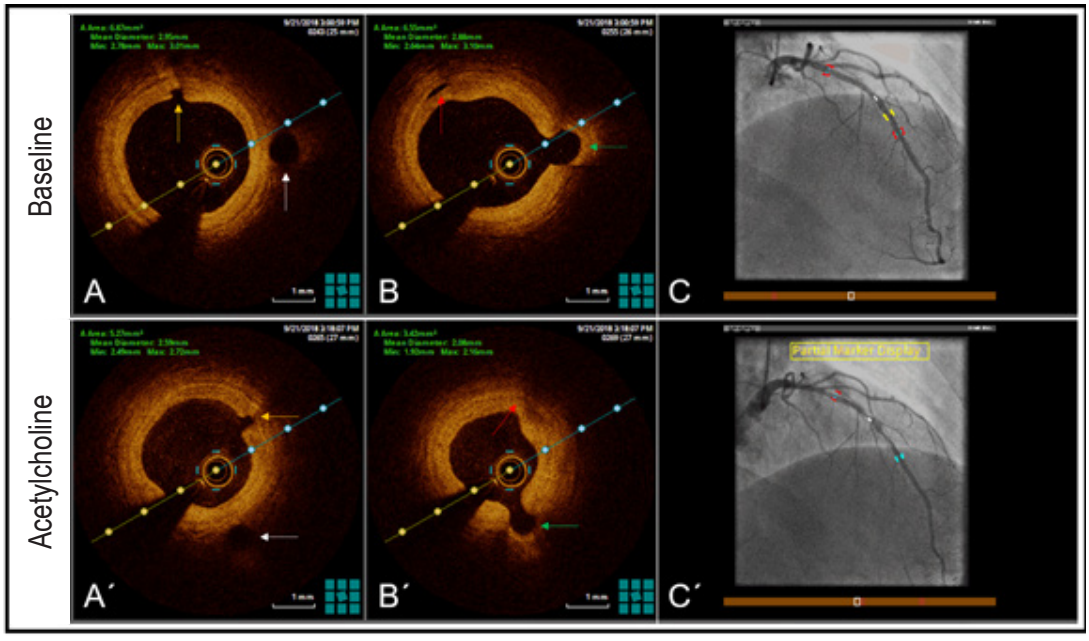

Figure 2 – *(A, B, C) Baseline images obtained by angiography and OCT. (A´, B´, C´) Angiography and OCT findings at the same cross-section after maximum dose of acetylcholine. Color arrows point side-branches before and after testing.*

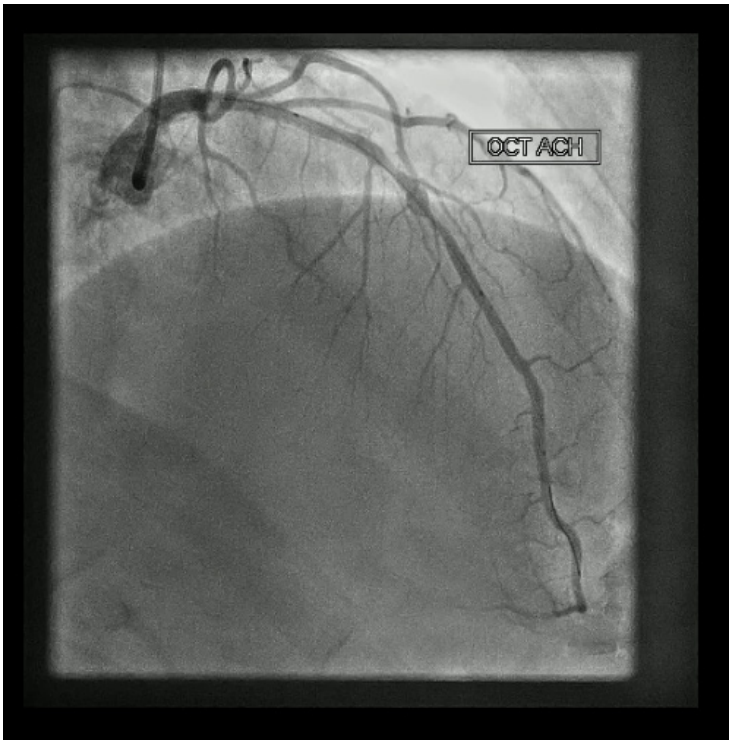

Video 2 – *Coronary angiography showing a LAD spasm -including the scaffolded segment- after peak dose of acetylcholine. Access the video at the link: http://abccardiol.org/supplementary-material/2021/11601/2019-0783-video2.mp4*

References

1. Ormiston JA, Serruys PW, Regar E, Dudek D, Thuesen L, Webster MW, et al. A bioabsorbable everolimus-eluting coronary stent system for patients with single de-novo coronary artery lesions (ABSORB): a prospective open-label trial. Lancet. 2008;371(9616):899-907.
2. Byrne RA, Stefanini GF, Capodanno D, Onuma Y, Baumbach A, Escaned J, et al. Report of an ESC-EAPCI Task Force on the evaluation and use of bioresorbable scaffolds for percutaneous coronary intervention: executive summary. EuroIntervention. 2018;39(18):1591-601.
3. Serruys PW, Ormiston JA, Onuma Y, Regar E, Gonzalo N, Garcia-Garcia HM, et al. A bioabsorbable everolimus-eluting coronary stent system (ABSORB): 2-year outcomes and results from multiple imaging methods. Lancet. 2009;373(9667):897-910.
4. Onuma Y, Dudek D, Thuesen L, Webster M, Nieman K, Garcia-Garcia HM, et al. Five-year clinical and functional multislice computed tomography angiographic results after coronary implantation of the fully resorbable polymeric everolimus-eluting scaffold in patients with de novo coronary artery disease: the ABSORB cohort A trial. JACC Cardiovasc Interv. 2013;6(10):999-1009.
5. Ellis SG, Kereiakes DJ, Metzger DC, Caputo RP, Rizik DG, Teirstein PS, et al. Everolimus-Eluting Bioresorbable Scaffolds for Coronary Artery Disease. N Engl J Med. 2015;373(20):1905-15.
6. Serruys PW, Chevalier B, Dudek D, Cequier A, Carrie D, Iniguez A, et al. A bioresorbable everolimus-eluting scaffold versus a metallic everolimus-eluting stent for ischaemic heart disease caused by de-novo native coronary artery lesions (ABSORB II): an interim 1-year analysis of clinical and procedural secondary outcomes from a randomised controlled trial. Lancet. 2015;385(9962):43-54.
7. Serruys PW, Onuma Y, Garcia-Garcia HM, Muramatsu T, van Geuns RJ, de Bruyne B, et al. Dynamics of vessel wall changes following the implantation of the absorb everolimus-eluting bioresorbable vascular scaffold: a multi-imaging modality study at 6, 12, 24, 36 months. EuroIntervention.2014;9(11):1271-84.
8. Serruys PW, Chevalier B, Sotomi Y, Cequier A, Carrie D, Piek JJ, et al. Comparison of an everolimus-eluting bioresorbable scaffold with an everolimus-eluting metallic stent for the treatment of coronary artery stenosis (ABSORB II): a 3 year, randomised, controlled, single-blind, multicentre clinical trial. Lancet. 2016;388(10059):2479-91.
9. Goncalves-Ramírez LR, Gutiérrez H, Cortés C, Gómez I, San Román JA, Amat-Santos IJ. Functional and structural coronary recovery at the 5-year follow-up after bioresorbable vascular scaffold implantation. An optical coherence tomography analysis. RevEspCardiol.2019;72(4):357-9.
10. Goncalves-Ramírez LR, Gutiérrez H, Rojas P, Cortés C, Serrador A, Ramos B, et al. Fully bioresorption of an Absorb bioresorbable vascular scaffold after scaffold restenosis. Cardiol J.2019;26(2):209-211.

Pericardial Masses: A Rare Presentation of Tuberculous Pericarditis Documented by 3D Echocardiography

Alex dos Santos Felix,[1] Viviane Belidio Pinheiro da Fonseca,[1] Rodrigo Coelho Segalote,[1] Larissa Franco de Andrade,[1] Deborah Louize da Rocha Vianna Palmieri,[1] Ana Paula dos Reis Velloso Siciliano[1]

Instituto Nacional de Cardiologia,[1] Rio de Janeiro, RJ – Brazil

Learning Points

• Pericardial masses are frequently caused by metastatic or primary tumors, but may be rarely caused by inflammatory, infectious or granulomatous diseases such as tuberculous pericarditis.

• In severe cases, with large effusion and hemodynamic impairment (pericardial tamponade), drainage is mandatory, and the gold-standard management includes pericardiotomy with complete drainage and mass resection to achieve a better therapeutic result, contribute to diagnosis and avoid fluid re-accumulation.

• Multimodality imaging and the use of 3D echocardiography to better depict details of the mass, its attachment to adjacent structures and to evaluate other thoracic and mediastinal structures is greatly valuable to clarify the correct etiology and exclude differential diagnoses.

Introduction

Pericarditis is a rare manifestation of tuberculosis (TB) that, despite occurring in only 2% of cases,[1] is responsible for approximately 70% of all cases of large pericardial effusion and most cases of constrictive pericarditis in developing countries. Pericardial masses are very rare presentations of TB, and can be mistaken as primary or metastatic pericardial tumors. That being said, there should be a prompt and careful evaluation to rule out underlying malignancy.

Case Report

A 29-year-old male was admitted to the Emergency Room with orthopnea and peripheral edema, reporting progressive dyspnea over the last two weeks, after protracted low fever, arthralgia, and weight loss (16 kg) over the last five months. The patient did not have a history of cardiovascular or pulmonary diseases. Primary examination showed tachycardia, signs of respiratory distress, regular pulse, and hypophonic heart sounds. Hepatomegaly and peripheral edema 2+/4+ were noted, and all other clinic aspects were normal.

Investigation

Electrocardiography showed low QRS voltage and tachycardia. In laboratory tests, increased C-reactive protein (9.72 mg/L) stood out. Leukocyte count was normal and hemocultures were all negative.

The suspicion was pericardial tamponade, and a transthoracic echocardiogram (TTE) was performed. A large pericardial effusion was detected, with increased respiratory variation in peak E-waves velocity in mitral (>25%) and tricuspid inflow (>50%), dilated inferior vena cava (IVC) with increased hepatic vein expiratory flow reversal, pointing to diastolic restriction. Additionally, echocardiography showed a thickened pericardium with surface irregularities and two large intrapericardial masses with regular contours, measuring 5.5x2.0cm and 4.3x2.3cm, interconnected by a bridge of tissue, attached to visceral and parietal layers of the pericardium by fibrinous strands, floating inside the pericardial fluid and not invading surrounding tissues, better depicted by 3D analysis (Figure 1, Videos 1-2). Biventricular systolic function was normal. A thoracic computed tomography (CT) scan showed mediastinal lymph node enlargement and no lesions in the lung parenchyma.

Treatment and Outcome

Empirical treatment for TB with oral rifampin (R), isoniazid (H), pyrazinamide (Z), and ethambutol (E) was started and, because of hemodynamic instability, the patient underwent urgent pericardiotomy. Serosanguinous drainage (600 ml) was performed and the masses were completely excised (Figure 2-A, Video 3). The masses were disc-shaped and macroscopically composed by a lobulated yellowish soft tissue. A specimen from the mass was submitted to intraoperative frozen section (IFS), ruling out malignancy. Histopathology revealed a pattern of chronic granulomatous inflammation with necrosis, consistent with TB (Figure 2-B).

The patient was discharged from hospital on oral RHZE and prescription for two months, followed by RH for four more months, without any complications or relapses and showing good outcome.

Discussion

Tuberculous pericarditis is an uncommon presentation of TB, occurring in only 2% of cases.[1] It is usually caused by retrograde spread of *Mycobacterium tuberculosis bacilli* from peritracheal, peribronchial or mediastinal

Keywords

Heart Neoplasms/surgery; Pericarditis,Tuberculous/physiopathology; Cardiac Tamponade/surgery; Echocardiography,Three-Dimensional/methods; Diagnosis. Imaging/methods.

Mailing Address: Alex dos Santos Felix •
Instituto Nacional de Cardiologia - Rua das Laranjeiras, 374.
Postal Code 20521-290, Rio de Janeiro, RJ – Brazil
E-mail: alexsfelix@gmail.com
Manuscript received December 10, 2019, revised mnauscript January 22, 2020, accepted January 22, 2020

DOI: https://doi.org/10.36660/abc.20190876

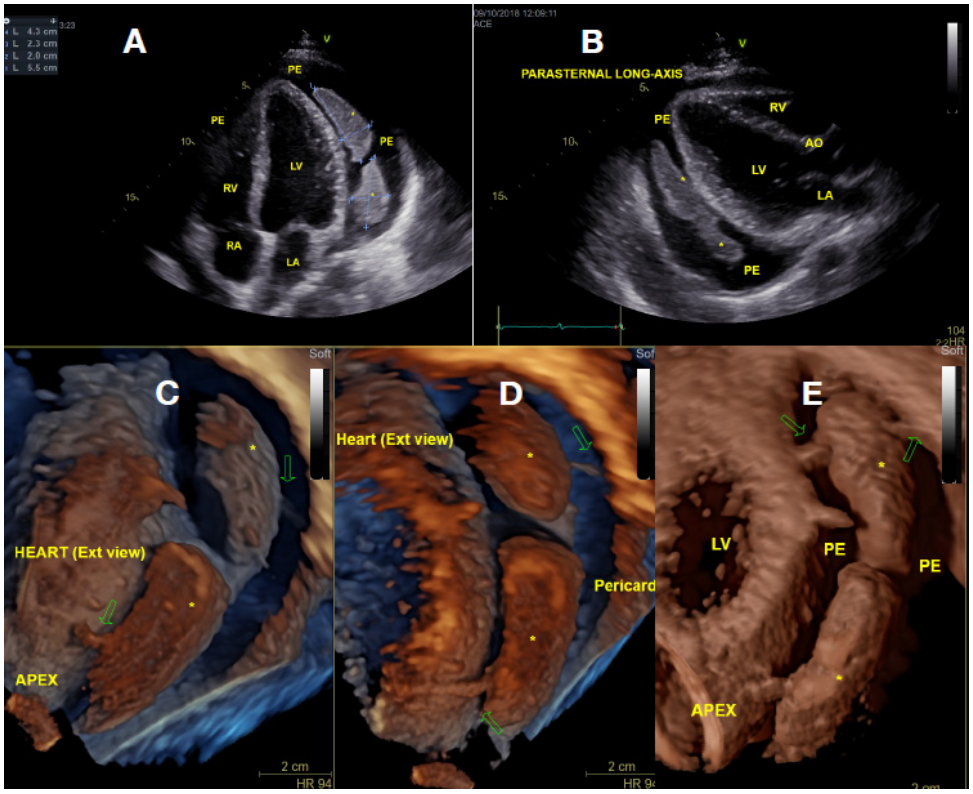

Figure 1 – *Transthoracic echocardiogram (TTE), showing large pericardial efusion with two intrapericardial masses (*). Two discoid masses were detected by 2D TTE, measuring 5.5 x 2.0cm and 4.3 x 2.3cm in its major diameters, from apical (A) and parasternal views (B). Rendered 3D images were obtained by post processing of datasets obtained by 3DTTE. Oblique 3D views in C, D and E show morphologic details of the masses, which are attached to visceral and parietal pericardial layers by fibrinous strands (arrows), floating inside the pericardial fluid, without invasion of surrounding tissues. LV: Left ventricle; RV: Right ventricle; LA: Left atrium; RA: Right atrium; PE: Pericardial effusion.*

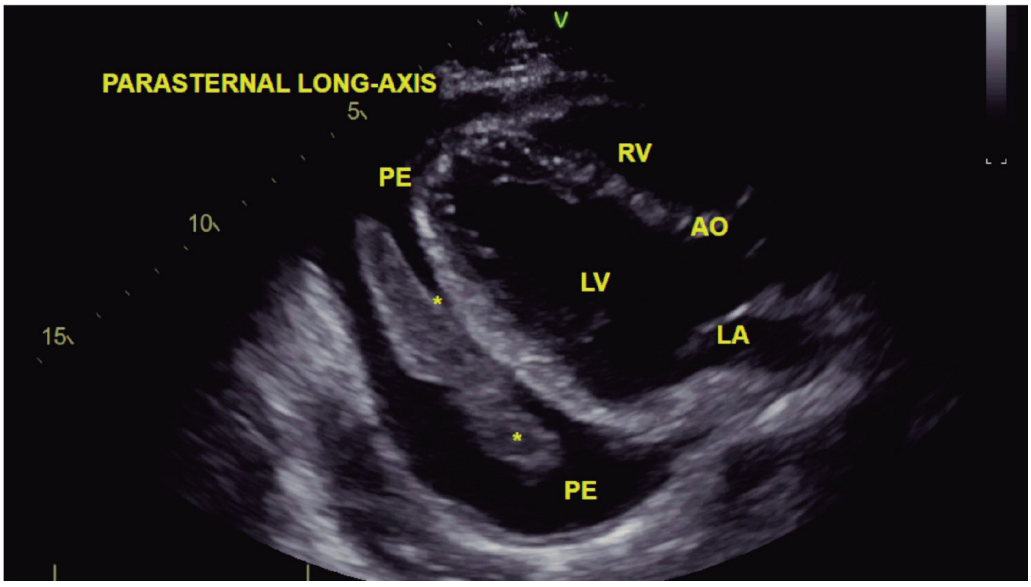

Video 1 – *Transthoracic Echocardiogram from apical 4 chamber and parasternal views, showing two disc-shaped intrapericardial masses floating inside large pericardial effusion. LV: Left ventricle; RV: Right ventricle; LA: Left atrium; RA – Right atrium; PE: Pericardial effusion.*
Access the video at the link: http://abccardiol.org/supplementary-material/2021/11601/2019-0876-video1.mp4

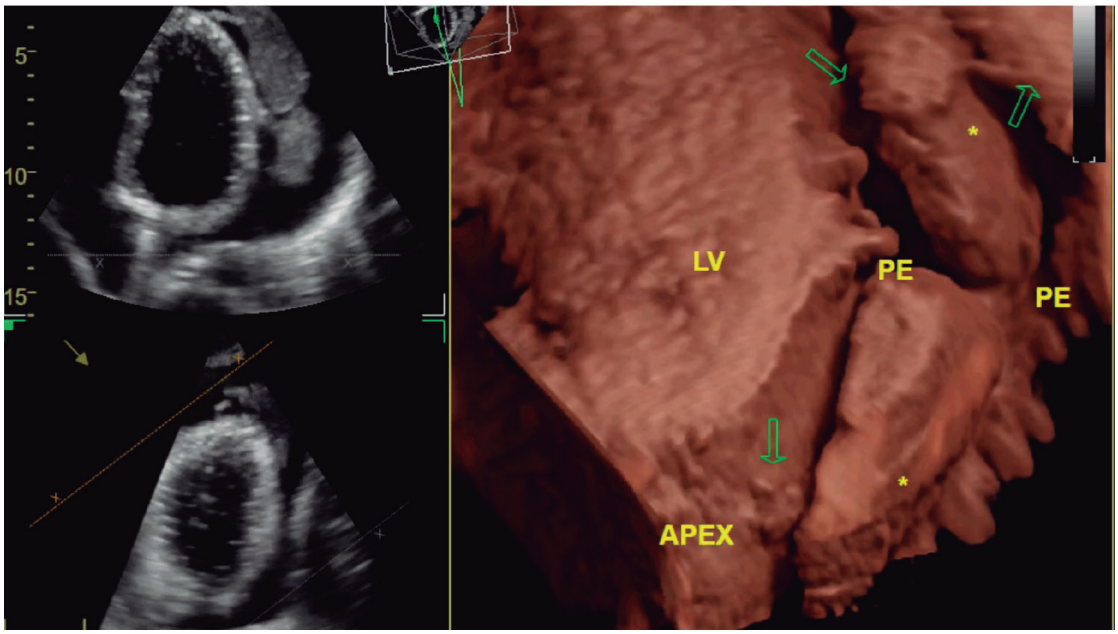

Video 2 – *3D rendered images from a dataset acquired from transthoracic echocardiogram, showing in oblique views a thickened pericardium with surface irregularities and two large intrapericardial masses with regular contours, interconnected by a bridge of tissue, attached to visceral and parietal layers of the pericardium by fibrinous strands, floating inside the pericardial fluid and not invading surrounding tissues. LV: Left ventricle; RV: Right ventricle; LA: Left atrium; RA: Right atrium; PE: Pericardial effusion. Access the video at the link: http://abccardiol.org/supplementary-material/2021/11601/2019-0876-video2.mp4*

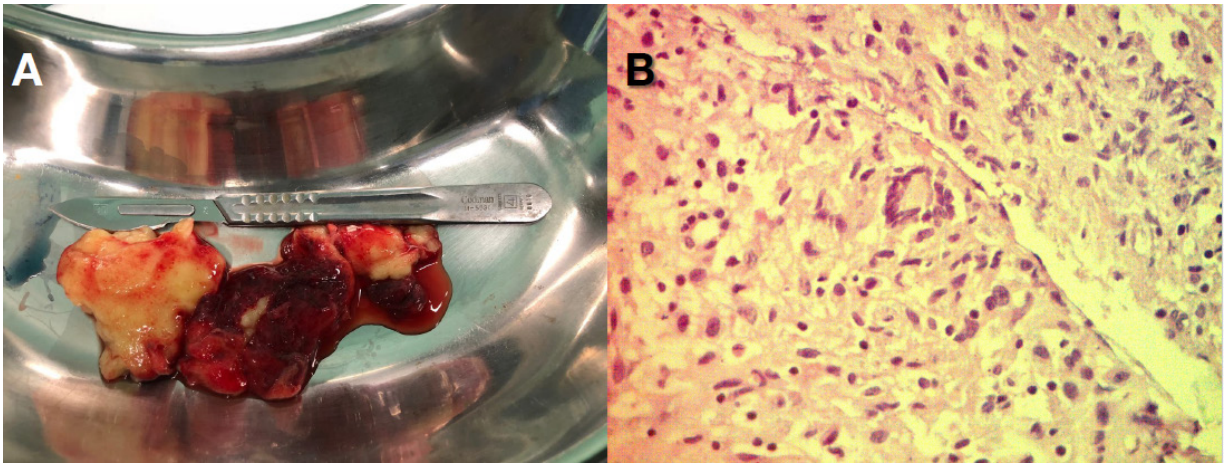

Figure 2 – *Histopathologic analysis of the intrapericardial masses. Macroscopically (A) the masses were disc-shaped and constituted by a lobulated yellowish soft tissue. In B, histopathological analysis with hematoxylin/eosin stain (magnification 40x) shows a pattern of chronic granulomatous inflammation with necrosis, consistent with tuberculosis granuloma.*

lymph nodes, or by hematogenous spread from primary tuberculous infection.[2]

Pericardial masses are relatively rare, mostly caused by malignancies, and the metastatic involvement of the pericardium is more frequent than primary tumors, often carrying a poor prognosis.[3] Inflammatory and infectious diseases are very rarely reported as causes of pericardial masses in the literature, with few reports of cardiac echinococcosis,[4] rheumatoid arthritis,[5] inflammatory pseudotumors,[6] and tuberculous pericarditis.[7] The presentation varies and patients are often asymptomatic, with pericardial involvement detected only at the autopsy or as an incidental finding during thoracic imaging tests. Some patients, however, may develop progressive symptoms of venous congestion due to evolution of pericardial effusion (diastolic restriction) or constriction, presenting with dyspnea, orthopnea, and peripheral edema.[8]

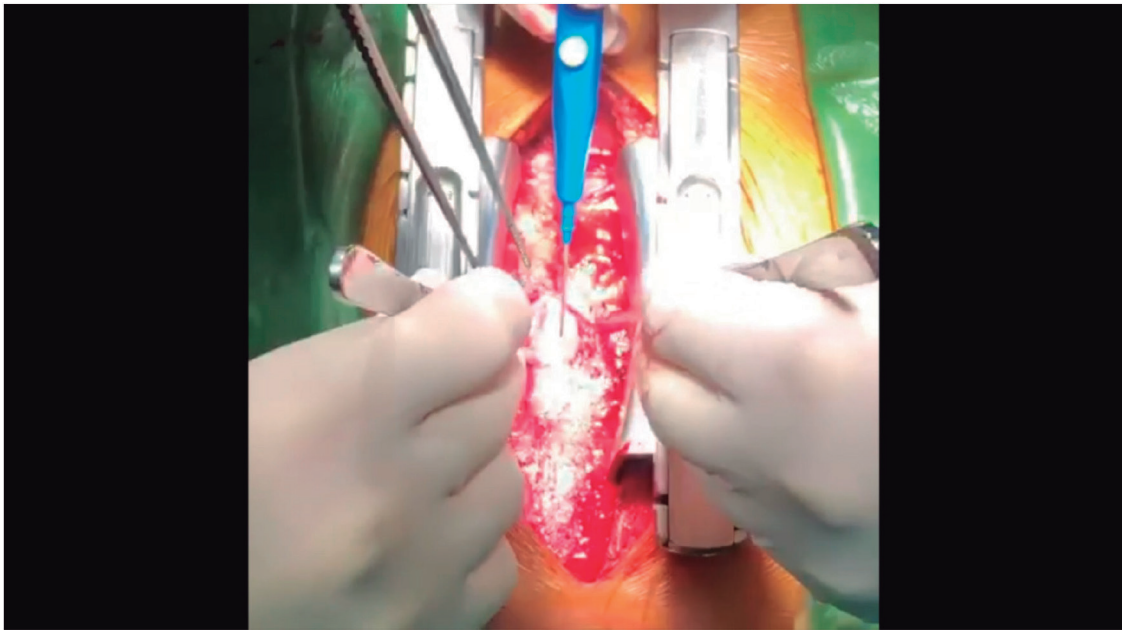

Video 3 – *Intraoperative images (surgical view). The patient underwent urgent pericardiotomy. A large volume of serosanguinous fluid under pressure was drained (600 ml), and complete excision of fibrinous strands and masses were performed.*
Access the video at the link: http://abccardiol.org/supplementary-material/2021/11601/2019-0876-video3.mp4

In severe cases, cardiac tamponade and cardiogenic shock may occur, which requires urgent intervention for fluid drainage and/or pericardiectomy.

In this report, we described a case of tuberculous pericarditis with large pericardial effusion and two large discoid masses floating inside the pericardial fluid and with attachments to pericardial parietal and visceral layers, well depicted with 3D TTE images. Pericardial masses caused by TB are very rare, and only a few cases have been reported in the medical literature so far.[7,9-12] There are at least five similar cases of TB pericarditis associated to pericardial masses, four in pediatric patients and one in a 19-year-old man[9].

The pathophysiology of these masses is still poorly understood and suggested to be the result of a conglomerate of red blood cells and protein materials inside the pericardial fluid, secondary to TB pericarditis.[7] In our case, the histologic findings were somewhat different from this description, as we found a chronic granulomatous inflammatory process, which is a typical aspect of a TB granuloma. Our patient did not present with clinical TB pneumonia, and did not match the classical diagnostic criteria for TB pericarditis, as *tubercle bacilli* were not found in the pericardial fluid or in the histological specimens obtained from the excised pericardium and from the masses. However, the finding of a typical TB caseating granuloma upon microscopical examination stablished the final diagnosis.

Conclusion

Pericardial masses are a rare presentation of tuberculous pericarditis, with few cases reported so far. Timely diagnosis and early treatment are important for a good outcome, as well as multimodal imaging is fundamental for differential diagnosis with other sources of cardiac masses such as tumors. This case illustrates the additional value of multimodal imaging and the use of 3D echocardiography for an accurate diagnosis, thus providing important data for decision-making and an effective treatment strategy.

Author contributions

Conception and design of the research and Acquisition of data: Felix AS, Fonseca VBP, Segalote RC, Andrade LF, Palmieri DLRV, Siciliano APRV; Analysis and interpretation of the data: Felix AS, Segalote RC, Andrade LF, Palmieri DLRV, Siciliano APRV; Writing of the manuscript: Felix AS; Critical revision of the manuscript for intellectual content: Felix AS, Fonseca VBP, Siciliano APRV.

Potential Conflict of Interest

No potential conflict of interest relevant to this article was reported.

Sources of Funding

There were no external funding sources for this study.

Study Association

This study is not associated with any thesis or dissertation work.

References

1. Fowler NO. Tuberculous pericarditis. JAMA. 1991;266(1):99–103.
2. Commerford PJ, Strang JIG. Tuberculous pericarditis. In: Coovadia HM, Benatar SR, eds. A Century of Tuberculosis: South African Perspectives. Cape Town: Oxford University Press; 1991.p.123–36
3. Luk A, Ahn E, Vaideeswar P, Butany JW. Pericardial tumors. Semin Diagn Pathol. 2008;25(1):47-53.
4. Oliver JM, Sotillo JF, Domínguez FJ, Lopes de Sá E, Calvo L, Salvador A, et al. Two-dimensional echocardiographic features of echinococcosis of the heart and great blood vessels. Clinical and surgical implications. Circulation. 1988 Aug;78(2):327-37.
5. Cañas F, León JDLP, Gomez JE, Cañas CA. A giant fibrinoid pericardial mass in a patient with rheumatoid arthritis: a case report. Eur Heart. Case Reports.2019;3(2):1-5.
6. Blanco M, Fulquet E, Laguna G, Martinez G, Sevilla T, Di Stefano S, et al. Cardiac Inflammatory Myofibroblastic Tumor in a Young Male Patient With Myopericarditis. Circulation. 2015;132(25):e386–e387.
7. Yoon SA, Hahn YS, Hong JM, Lee OJ, Han HS. Tuberculous pericarditis presenting as multiple free floating masses in pericardial effusion. J Korean Med Sci. 2012;27(3):325-8.
8. Mady C, Fernandes F, Ohki F. Tumores do pericárdio. Rev Soc Cardiol Estado de São Paulo. 2011;21(1):38-41.
9. Li C, Zhao Q, Wu X, Yu J. Tuberculous pericarditis mimicking multiple tumors in pericardial effusion. J Int Med Res. 2019;47(5):2262-8.
10. Lin JH, Chen SJ, Wu MH, Lee PI, Chang CI. Fibrinofibrous pericarditis mimicking a pericardial tumor. J Formos Med Assoc. 2000;99(1):59-61.
11. Massoure PL, Boddaert G, Caumes JL, Gaillard PE, Lions C, Grassin F. Porridge-like tuberculous cardiac tamponade: treatment difficulties in the Horn of Africa. Gen Thorac Cardiovasc Surg. 2010;58(6):276-8.
12. Garg A, Rajamouli DS, Eknath JU, Vasant KJ. Tuberculous pseudotumor of the pericardium: a case report. Indian J Thorac Cardiovasc Surg. 2013;29:262-4.

Dilated Cardiomyopathy Reversibility in Sheehan's Syndrome: A Case Report

Maria Luíza Barbosa Fernandes Dourado,[1] Taís Paiva da Costa,[1] Márcia Sampaio de Carvalho,[1] Carlos Geraldo Guerreiro de Moura[1,2]

Obras Sociais Irmã Dulce,[1] Salvador, BA - Brazil

Escola Bahiana de Medicina e Saúde Pública,[2] Salvador, BA - Brazil

Introduction

Sheehan's syndrome, discovered in 1937 by Harold Leeming Sheehan is described as pan-hypopituitarism secondary to pituitary necrosis after post-partum hemorrhage.[1] The clinical condition presentation depends on the hormonal shortfall presented, and may involve changes in serum cortisol levels, thyroid function, growth hormones, breastfeeding and sex hormones.[2] Although poorly described in the literature, there are reports of dilated cardiomyopathy associated with Sheehan's syndrome, some with reversibility of cardiopathy after hormone replacement therapy. [3] This paper reports a clinical case of Sheehan's syndrome associated to dilated cardiomyopathy that displayed cardiac function improvement after hormone replacement therapy.

Case Report

The subject reported on this paper is about a 36-year-old female, married, housekeeper, from Inhambupe/BA, which had been admitted to a tertiary medical service with progressive dyspnea for 2 months that evolved to resting dyspnea at 02 days from admission. In addition, she reported lower limb edema and periorbital edema. Also complained about postprandial nausea and vomiting for 01 week with food remains, without mucus or blood, afebrile. Also referred asthenia, somnolence and mental confusion, with difficulty in the chronological organization of the facts. Thus, the patient had been treated with diuretic therapy in emergency, with partial improvement of dyspnea and pulmonary edema. She also reported previous hospitalization at age 18 due to complications caused by preeclampsia and post-partum hemorrhage, having no blood transfusions. She claimed post-partum agalactia and amenorrhea 18 years ago. The patient has an active sexual life with a single partner and doesn't use any contraceptive method. At physical examination, regular general state, with confused speech, hypoactivity and hypotension (ΔPAS 100-80 mmHg x ΔPAD 70-50 mmHg). Skin with reduced turgor and elasticity, presence of periorbital edema. The cardiovascular system displayed calm precordium, non-palpable and non-visible apical impulse, hypophonetic heart sounds, no blows, no extra heart sound. Perfused extremities with depressible edema + 1/4 +, cold, painless. Other follow-ups without changes.

Initial laboratory tests showed inadequately normal TSH in 4.93 μUI/mL (0.38-5.3) with free T4 under 0.4 ng/dL (0.5-1.2), normovolemic hyponatremia (sodium 133mEq/L - VR 136-144). Additional admission exams: hemoglobin 12 mg/dL, hematocrit 35.9%, leukogram 12,880: 89% segmented, 4% lymphocytes, 1% eosinophils and 6% monocytes; platelets 165,000/mm^3 and normal renal function.

The replacement of hydrocortisone 500 mg bolus was followed by low doses of levothyroxine (50 mcg/day). After introduction of hormonal therapy, the patient presented improvement of hypoactivity and asthenia presented on admission.

The clinical status and response to hormone therapy confirmed the diagnostic suspicion of hypopituitarism secondary to pituitary necrosis after post-partum hemorrhage; confirmed by the following tests: GH 0.1 ng/mL (0.5-3.6), beta-estradiol 20 pg/mL (<40 post-menopausal), FSH 4.5 mUI/mL (16 - 113: post-menopausal), LH 2.96 mIU/mL (10.8 - 58.6: postmenopausal), prolactin 3.36 ng/mL (2-15), ACTH 35.8 pg/mL (VR 7.2-63.3) and morning serum cortisol 1.5 mcg/dL (5.4-25). Brain's magnetic nuclear resonance revealed partial empty *sella turcica* with herniation of the suppressing cistern into the saddle, identifying a thin layer of the pituitary gland in the sealing floor, with homogeneous enhancement to the medium contrast (Figure 1).

Aware of dyspnea and cardiac sounds hypophonese status associated with edemigenic syndrome, a chest X-ray (Figure 2.A) and transthoracic echocardiography were requested. The radiograph pointed to cardiomegaly. The echocardiogram displayed dilated cardiomyopathy with significant left ventricular systolic dysfunction, at the expense of diffuse hypokinesia ventricular ejection fraction (LVEF) of 27%, and mild mitral regurgitation.

Once adjustments of the hormone therapy instituted were accomplished with levothyroxine 100 mcg/day and prednisone 10 mg/day, significant clinical and radiological (Figure 2B) improvement had been revealed. The serial echocardiogram after 2 weeks of treatment showed a 12% improvement in ejection fraction and reduction of global

Keywords

Hypopituitaris; Sheehan`s Syndrome; Cardiomyopathy, Dilated; Diagnostic, Imaging; Hormone Replacement Therapy.

Mailing Address: Maria Luíza Barbosa Fernandes Dourado •
Obras Sociais Irmã Dulce - Avenida Dendezeiros do Bonfim, 161. Postal Code 40420-415, Bonfim, Salvador, BA – Brazil
E-mail: mlbfdourado@gmail.com
Manuscript received August 14, 2019, revised manuscript December 22, 2019, accepted March 09, 2020

DOI: https://doi.org/10.36660/abc.20190547

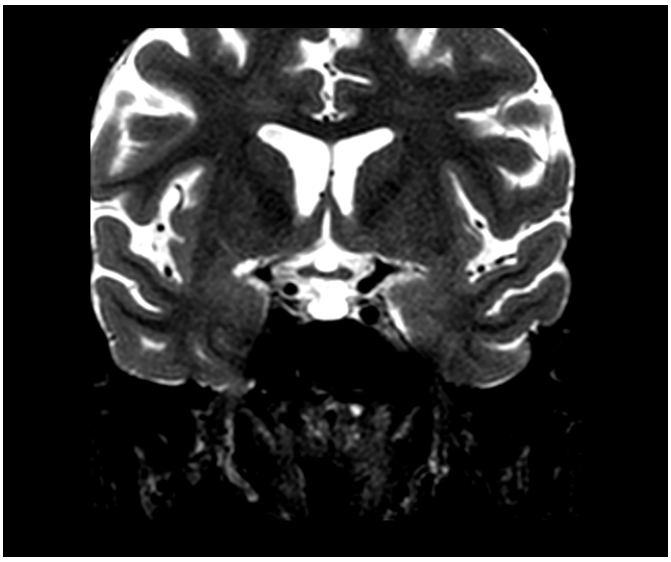

Figure 1 – *Magnetic resonance of the partial empty sella turcica.*

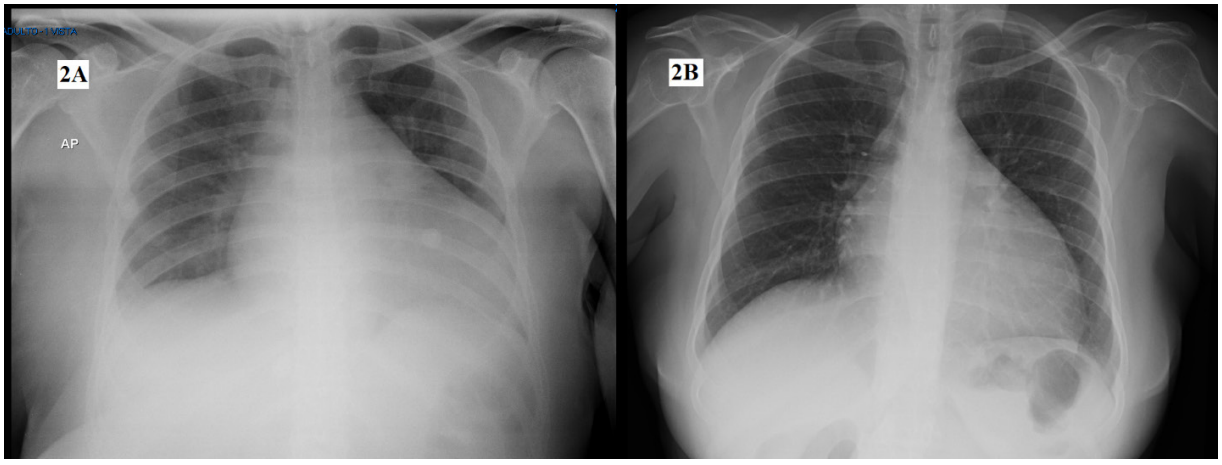

Figure 2 – *A) Chest radiography of hospital admission. B) Chest radiography after hormone therapy.*

systolic dysfunction even without specific therapy for congestive heart failure (CHF).

Heart failure therapy with reduced ejection fraction was only introduced a week before hospital discharge, as to date, the patient had borderline blood pressure levels. She was referred to the cardiology outpatient clinic with guidance on the use of cardioselective beta-blockers, in addition to spironolactone.

Discussion

Sheehan's syndrome incidence, secondary to peripartum hemorrhage, is directly related to quality of medical care during pregnancy.[4] Maternal mortality is an important marker of population's health status. One of the main causes of maternal mortality is post-partum hemorrhage with may have as a consequence the occurrence of pituitary necrosis.[5]

The clinical presentation of Sheehan's syndrome depends on the level of ischemia of pituitary's gland.[1] About 75% of pituitary's cells should be compromised to cause secondary hormone deficiency.[3] Signs and symptoms are divided into acute and chronic illnesses.[6] The acute ones consisted of hypotension, shock, tachycardia, hypoglycemia, hyponatremia, extreme fatigue, nausea and vomiting, classically represented by acute adrenal insufficiency. Chronically, patients may present asthenia, fatigue, muscle strength decrease, constipation, cold intolerance related to central hypothyroidism; reduction of libido, agalactia,

amenorrhea and infertility, due to gonadotrophic stimulus reduction; including psychiatric disorders.[1]

According to literature, the search for medical care is motivated by hydroelectrolytic disturbances, especially hyponatremia. During the first care given to the patient of the case, nausea, vomiting and hyponatremia directed the diagnostic and therapeutic approach. It was only possible to know patient's obstetric history after confusional status was solved. However, in the emergency context, the patient was admitted with edemigenic syndrome of cardiac etiology.

The presentation of Sheehan's Syndrome as CHF is atypical and cardiac involvement was considered the rarest among those described.[7] By 2013, Doshi et al.[3] had already mentioned the hypo-polyglandular entity associated to cardiac function reversibility. The cardiopathy of the patient with hypothyroidism is mainly associated with the pericardial effusion, when the ventricular filling time is reduced, sometimes resulting in cardiac tamponade.[8] When related to adrenal insufficiency, it is reported to patients with hypocortisolism as part of type 1 autoimmune polyglandular syndromes, also reversible after hormonal correction.[9] However, etiology of the dilated cardiomyopathy related to Sheehan's syndrome remains unknown.

The improvement of ventricular function demonstrated in the clinical status during the short period of two weeks was curious. There was an ejection fraction increase from 27% to 39% after two weeks of admission despite the use of formal heart failure's therapy. Other cases described in the literature expose the reversibility of dilated cardiomyopathy when associated with Sheehan's syndrome, however, most of them associating hormone replacement and CHF with LVEF's therapy.[7,9-12]

Doshi et al.[3] approached the clinical case of a 42-year-old female patient with an emergency presentation of secondary cardiogenic shock to pan-hypopituitarism due to Sheehan's syndrome. Amenorrheic 14 years ago (date of the last gestation), she was managed with glucocorticoids, levothyroxine and 48 hours of inotropic use. Six months after the therapy started, the patient had a 100% increase of LVEF (initial: 20%, follow-up: 40%), radiological parameters improvement and became asymptomatic. In 2014, in Saudi Arabia, the case of a young patient who was admitted to the emergency room presenting dyspnea and edemigenic syndrome for 6 months with a peripartum dilated cardiomyopathy diagnosis was studied. However, after extensive investigation, the initial diagnosis was reconsidered, since the patient had a history of peripartum hemorrhage, adrenal and thyroid insufficiency, as well as empty *sella turcica*. Thus, she was diagnosed with Sheehan's syndrome associated with dilated cardiomyopathy, reversed in 06 months after hormone replacement.[7]

It was concluded that Sheehan's syndrome associated with dilated cardiomyopathy is rare and there is no therapeutic approach described by literature. The hormone replacement for the deficiencies presented is the main known available resource, since the improvement of the clinical cases described is independent of the specific therapy for CHF with reduced ejection fraction. The main syndromes treated involve the replacement of thyroid hormone and corticoid therapy, and there is not a consensus about the benefit of GH replacement.[1]

Author contributions

Conception and design of the research, Acquisition of data and Analysis and interpretation of the data: Dourado MLBF, Costa TP, Carvalho MS; Statistical analysis: Dourado MLBF; Writing of the manuscript: Dourado MLBF, Costa TP; Critical revision of the manuscript for intellectual content: Dourado MLBF, Costa TP, Moura CGG.

Potential Conflict of Interest

No potential conflict of interest relevant to this article was reported.

Sources of Funding

There were no external funding sources for this study.

Study Association

This study is not associated with any thesis or dissertation work.

Ethics approval and consent to participate

This article does not contain any studies with human participants or animals performed by any of the authors.

References

1. Soares DV, Conceição FL, Vaisman M. Aspectos diagnósticos e terapêuticos da Síndrome de Sheehan. Arq Bras Endocrinol Metab. 2008; 52(5): 872-7.
2. Snyer PJ. Update. [Internet]. [Cited in 2018 Jun 12] Available from: https://www.uptodate.com/contents/clinical-manifestations-of-hypopituitarism?search=hipopituitarismo&source=search_result&selectedTitle=1~150&usage_type=default&display_rank=1
3. Doshi S, Roy A, Ramamoorthy A, Kothari SS, Bahl VK. Dilated Cardiomyopathy. Circ Heart Fail. 2013; 6:e-19-e-21.
4. Organização Pan-Americana da Saúde. (OPAS). Manual de orientação para o curso de prevenção e manejo obstétrico da hemorragia: Zero Morte Materna por Hemorragia. Brasília; 2018.
5. Vieira AEF, Rocha MMD. Síndrome de Sheehan. Relato de caso e revisão da literatura. Rev Bras Med. 2011;14(4):105-8.
6. Molitch ME. Pituitary diseases in pregnancy. Semin Perinatol. 1998; 22(6):457-70.
7. Islam AKMM, Hasnat MA, Doza F, Jesmin H. Sheehan's syndrome with reversible dilated cardiomyopathy: a case report and brief overview. J Saudi Heart Assoc. 2014; 26(2):117-20.

8. Barisic Júnior S, Barisic GFT, Markman Filho B. Cardiopatias e tireoide. Rev Bras Clin Ter. 2006;63(3):127-33.

9. Natarajan V, Asha HS, Paul T, Sunithi MD. Sheehans syndrome with reversible cardiomyopathy. OA Case Reports. 2014; 3(5):44.

10. Joshi A, Yonzon I. Sheehan's syndrome associated with reversible dilated cardiomyopathy in na elderly Nepalese woman. Nepal Med Coll. 2015; 17 (3-4):185-6.

11. Ikegami Y, Fukuda T, Jo R, Momiyama Y. Reversible Cardiomyopathy Accompanied by Secondary Adrenal Insufficiency. Circ Heart Fail. 2016; 9(3):e002919.

12. Bhat MH, Bagdadi F, Rafi A Shah PA. Reversible cardiomiopathy as a rare presentation os sheehan's syndrome case report and review of literature. Int J Adv Med. 2017; 4(6): 1713-5.

Systematic Staged Percutaneous Balloon Pulmonary Angioplasty in Severe Inoperable Chronic Thromboembolic Pulmonary Hypertension

Kazuhiro Dan,[1] *Akira Shionoda,*[1] *Hiromi Matsubara*[2]
Ichinomiya Nishi Hospital,[1] *Ichinomiya - Japan*
Okayama Medical Center,[2] *Okayama - Japan*

Introduction

The treatment for chronic thromboembolic pulmonary hypertension (CTEPH) is limited to pulmonary endarterectomy (PEA), drug therapy, and percutaneous balloon pulmonary angioplasty (BPA).[1] The gold-standard treatment is PEA, and patients with CTEPH and proximal lesions are generally good surgical candidates. Perioperative complications and persistent pulmonary hypertension due to incomplete endarterectomy or secondary vasculopathy are typical problems after the procedure.[2] A meta-analysis has shown that the efficacy of drug therapy for severe CTEPH is limited, and many patients do not achieve sufficiently reduced pulmonary artery (PA) pressure, even if exercise tolerance is marginally improved.[3] Percutaneous BPA was first reported in 2001, but its safety was not proven at that time.[4] As recently as one decade ago, pulmonary hypertension was first associated with poor prognosis. Fortunately, treatments for pulmonary hypertension have dramatically improved ever since, particularly for patients with CTEPH. BPA is still a challenging strategy, limited to a specific operator and facility, but its results have been improving.[5]

Case Report

A 76-year-old female patient (height 1.45 m, weight 40 kg) presented to the service with a three-month history of dyspnea on exertion. She had no history of deep vein thrombosis or acute pulmonary embolism. One week before admission, her dyspnea worsened (New York Heart Association class IV), she developed leg edema and became unable to walk. On admission, her blood pressure was 210/95 mmHg, heart rate was 85 bpm, SpO_2 80% (room air), and respiratory rate was 32 breaths per minute. An electrocardiogram showed sinus rhythm and right ventricular hypertrophy (RVH) (Figure 1A). Laboratory exams showed creatinine level at 0.84 mg/dl, hemoglobin level at 17.4 g/dl, and brain natriuretic peptide (BNP) level at 1000 pg/ml. No evidence of collagen vascular disease was noted. A transthoracic echocardiography revealed right heart failure [right atrium and ventricle dilatation; estimated systolic PA pressure of 58 mmHg; 6% right ventricular fractional area change; pericardial effusion] with preserved left ventricular contraction (ejection fraction: 65%) (Figure 1B).

She underwent right heart catheterization, which revealed PA pressure of 60/38 (47) mmHg, pulmonary artery wedge pressure (PAWP) of 6 mmHg, cardiac index of 2.17 L/min and pulmonary vascular resistance index of 18.89 Wood unit•m^2. Coronary angiography was normal. Contrast-enhanced chest computed tomography scan showed no evidence of acute pulmonary embolism (Figure 1D-F). PA angiography revealed webs, and subtotal and total occlusion lesions in bilateral segmental to subsegmental pulmonary arteries (Figure 2A). Lung perfusion scintigraphy showed multiple bilateral defects (Figure 3A).

The patient was put on continuous infusions of heparin and low-dose dobutamine over a month; however, her condition did not improve and she was diagnosed with CTEPH. Until three months before admission, she independently performed all activities, but being elderly and frail, she reported being completely bedridden for one week prior to admission. Her frailty (Canadian clinical scale 8) and multiple distal lesions rendered her a poor operative candidate, so the medical staff decided to perform BPA, as this is a less-invasive and lower-risk treatment, after discussions with a cardiac surgeon.

The target vessels were right (A1, A2, A3, A5, A7, and A8) and left pulmonary arteries (A 3, A4, A6, and A10). The procedure was performed using a 0.014-inch guidewire system, similar to a percutaneous coronary intervention. A 6 French Amplatz left catheter was directed into a branch of the PA via the right femoral vein. The wiring was performed with two kinds of low-weight guidewire (B-pahm 0.6g, Japan Lifeline, Tokyo, Japan) (Chevalier Floppy 2g, FMD, Tokyo, Japan), supported by a balloon catheter (BC). In the first procedure, BPA was initiated from the anterior part (Right A3 and A5 Left A3.) using a 2.0-mm semicompliant BC (Ikazuchi PAD, Kaneka, Osaka, Japan). Additional BPA using a 2.0-mm BC was performed on the posterolateral portion (Right A3, A5, A7 and A8. Left A4, A6 and A10.) one month later. Two months after that, we expanded all pre-dilated arteries using a 3.0-mm BC (Figure 2B and 2C). BPA was completed without intravascular imaging guidance and without complications such as lung injury and hemoptysis. We were not able to open the completely occluded arteries (Right A 1 and A2); however, her PA pressure decreased to 42/16 (26) mmHg immediately after the final BPA, and the mean PA pressure finally improved to 20 mmHg without hypoxemia (SpO_2 96%, room air). A new lung perfusion scintigraphy showed improved perfusion, with adequate pulmonary circulation over two-thirds of the total PA vascular bed (Figure 3B). She could ambulate independently and was discharged from the hospital. On discharge, her six-minute

Keywords

Angioplasty, Balloon, Pulmonary; Hypertension, Pulmonary; Pulmonary Embolism; Aging; Fragility.

Mailing Address: Kazuhiro Dan •
Ichinomiya Nishi Hospital - Kaimei-hira 1, Ichinomiya, Aichi 494-0001, Ichinomiya 4940001- Japan
E-mail: dan27k@gmail.com
Manuscript received October 17, 2019, revised mnauscript January 27, 2020, accepted March 16, 2020

DOI: https://doi.org/10.36660/abc.20190717

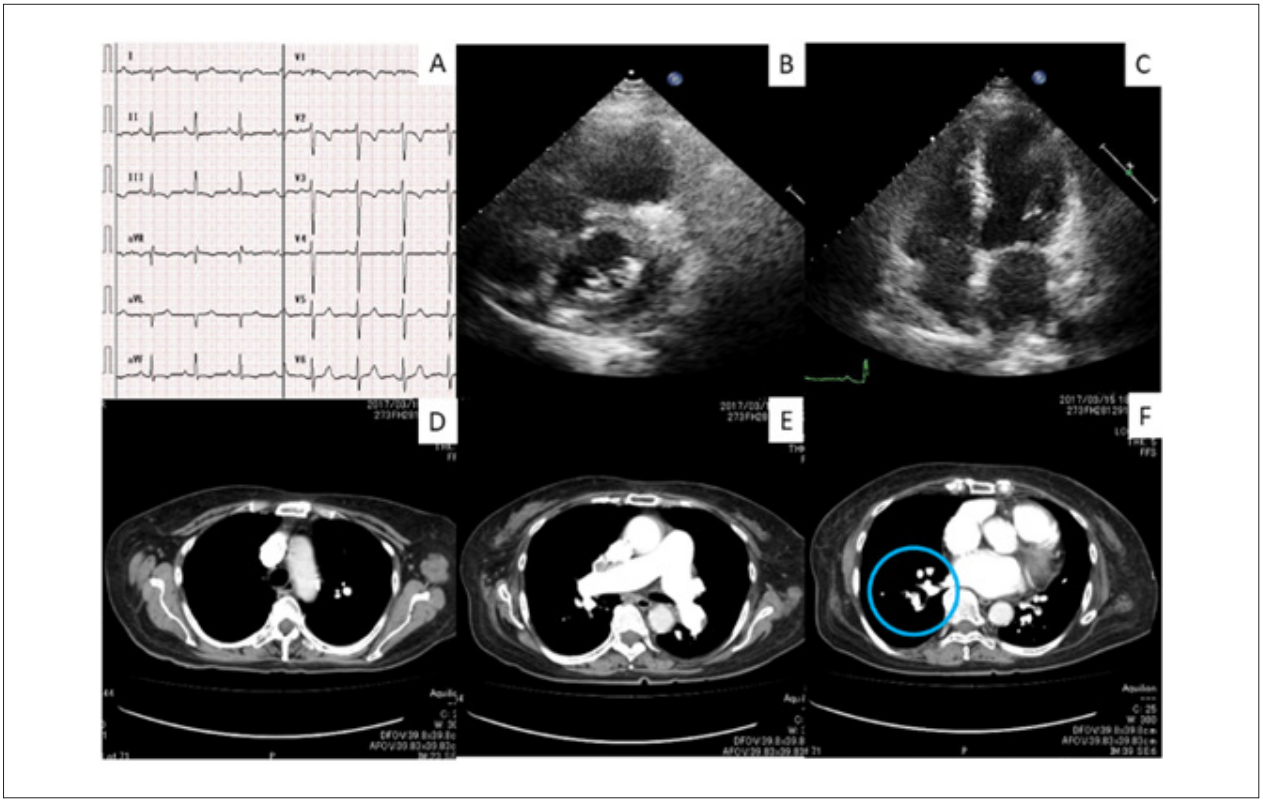

Figure 1 - *Physiological and radiological examinations before balloon pulmonary angioplasty. A) Electrocardiogram on admission showed S-I and T-III. B and C) Transthoracic echocardiography (end diastolic phase) showing right heart failure (B) upon admission, and right heart failure normalized two year after BPA (C). D-F) Contrast-enhanced chest computed tomography showing the avascular area in the right upper lobe (D), no evidence of acute pulmonary embolism in main pulmonary artery (E), and web-like finding in the right pulmonary artery branch 8 (blue circle in F).*

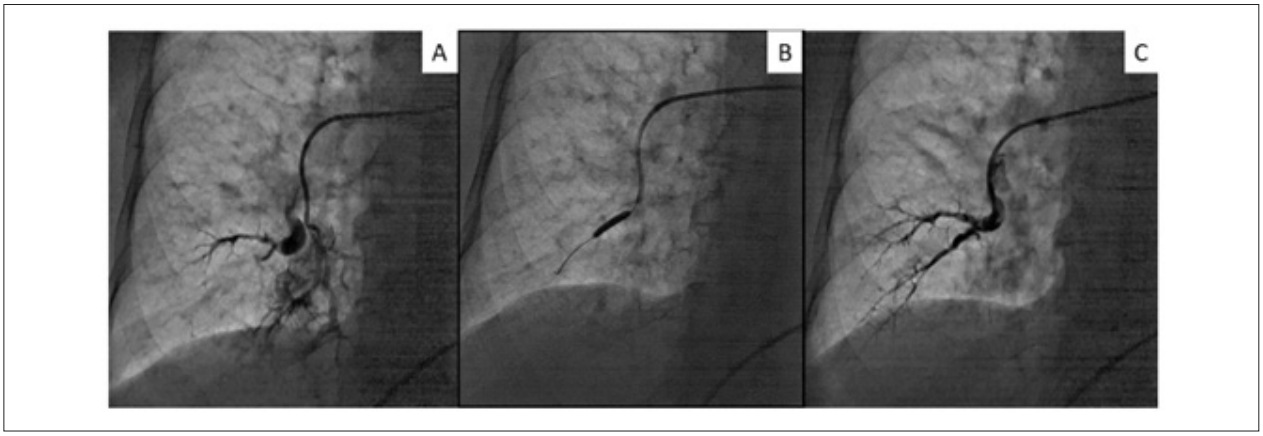

Figure 2 - *A representative pulmonary artery angiography in systematic staged balloon pulmonary angioplasty. A: Occluded right pulmonary artery (branch 8) detected by selective angiography. B: BPA with a 3.0-mm semicompliant balloon catheter. C: Final selective pulmonary angiography after systematic staged BPA with 2.0- and 3.0-mm semicompliant balloon catheters.*

walking distance was 236 m. She was prescribed supplemental oxygen, anticoagulants, and a low-dose diuretic drug. Her BNP decreased to 64 pg/ml. The right atrial and ventricular dilatations normalized on echocardiography (Figure 1C). Ever since, the patient has maintained a good clinical picture over the course of two years, but further monitoring is recommended.

Discussion

Our patient presented with severe inoperable CTEPH without thrombi at the main part of pulmonary arteries on computed tomography scan. Pulmonary angiography showed occluded pulmonary segmental arteries (right A 1, 2, 8 and left A 10) and arterial webbing in other segmental or subsegmental arteries.[6]

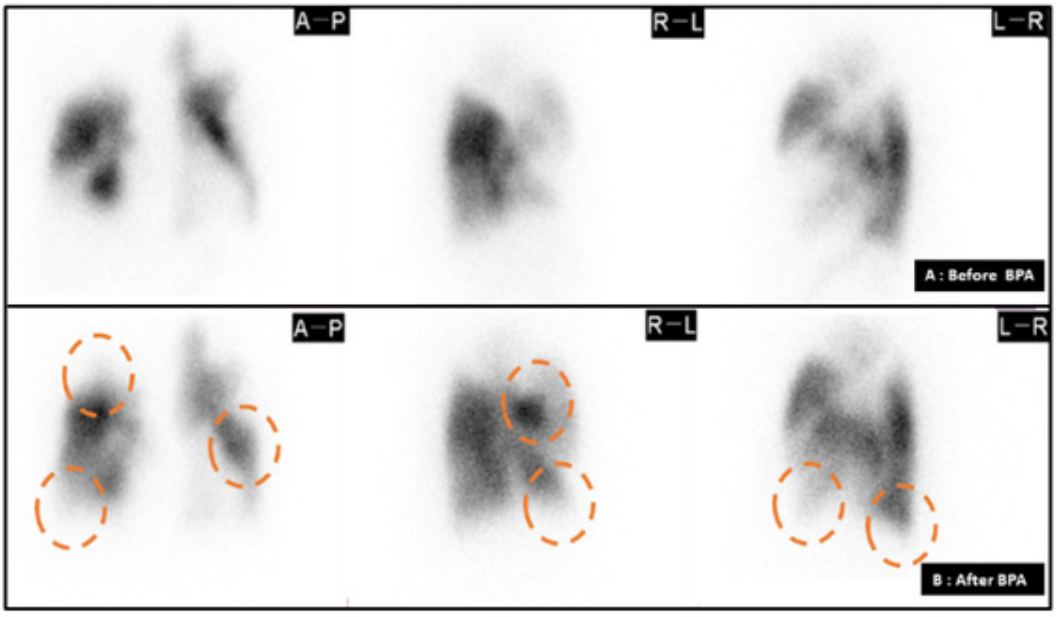

Figure 3 - *Lung perfusion scintigraphy before and after systematic balloon pulmonary angioplasty. A and B) Lung perfusion scintigraphy prior to (A) and after (B) BPA. Orange circles show improved perfusion areas.*

In this case, we performed three separate BPA sessions; however, more spaced sessions may be acceptable depending on the frailty and general condition of the patient in order to avoid lung injury (such as bleeding) due to pulmonary vessel injury.[1,7] We also considered ventilation-perfusion mismatch and started the procedure from the anterior part to improve hypoxemia. Occlusive lesions are a predictor of BPA-related complications.[8] We then proceeded with treating incompletely occluded arteries, once BPA-related complications may critically worsen the patient's hemodynamics and respiratory condition. A small BC (2.0 mm) was selected to avoid high-pressure incoming blood flow and then the multiple target arteries were dilated.

After dilation by incoming blood flow for two months from initial BPA, all treated arteries were dilated using a 3.0-mm BC, as per the anatomical diameter of PA. A recent report described that patients with CTEPH present increased arterial stiffness.[9] High systemic blood pressure is uncommon in CTEPH, but, in the present case, it was normalized after BPA.

Japanese groups have reported improved long-term outcomes associated with BPA for patients with CTEPH and distal lesions.[10] Further prospective observational studies and randomized controlled trials are required to compare BPA and drug therapy in patients with inoperable CTEPH, thus determining the efficacy of the procedure.

Conclusion

Systematic staged BPA, a treatment from anterior to posterior PA by two balloon catheters with different diameters (2.0 mm and 3.0 mm), can be safely performed even in inoperable patients with severe physical conditions. Nowadays, BPA may not be the last resort, but rather the first-choice treatment for the inoperable CTEPH population.

Author contributions

Conception and design of the research, Analysis and interpretation of the data and Writing of the manuscript: Dan K; Acquisition of data: Shionoda A; Critical revision of the manuscript for intellectual content: Matsubara H.

Potential Conflict of Interest

No potential conflict of interest relevant to this article was reported.

Sources of Funding

There were no external funding sources for this study.

Study Association

This study is not associated with any thesis or dissertation work.

Ethics approval and consent to participate

This article does not contain any studies with human participants or animals performed by any of the authors.

References

1. Kim NH, Delcroix M, Jais X, Madani MM, Matsubara H, Mayer E, et al. Chronic thromboembolic pulmonary hypertension. Eur Respir J. 2019;53(1):1801915.
2. Mayer E, Jenkins D, Lindner J, D'Armini A, Kloek J, Meyns B, et al. Surgical management and outcome of patients with chronic thromboembolic pulmonary hypertension: results from an international prospective registry. J Thorac Cardiovasc Surg. 2011;141(3):702-10.
3. Phan K, Jo HE, Xu J, Lau EM. Medical Therapy Versus Balloon Angioplasty for CTEPH: A Systematic Review and Meta-Analysis. Heart Lung Circ. 2018;27(1):89-98.
4. Feinstein JA, Goldhaber SZ, Lock JE, Ferndandes SM, Landzberg MJ. Balloon pulmonary angioplasty for treatment of chronic thromboembolic pulmonary hypertension. Circulation. 2001;103(1):10–3.
5. Mizoguchi H, Ogawa A, Munemasa M, Mikouchi H, Ito H, Matsubara H. Refined balloon pulmonary angioplasty for inoperable patients with chronic thromboembolic pulmonary hypertension. Circ Cardiovasc Interv. 2012;5(6):748-55.
6. Kawakami T, Ogawa A, Miyaji K, Mizoguchi H, Shimokawahara H, Naito T, et al. Novel Angiographic Classification of Each Vascular Lesion in Chronic Thromboembolic Pulmonary Hypertension Based on Selective Angiogram and Results of Balloon Pulmonary Angioplasty. Circ Cardiovasc Interv. 2016;9(10):e003318.
7. Ejiri K, Ogawa A, Fujii S, Ito H, Matsubara H. Vascular Injury Is a Major Cause of Lung Injury After Balloon Pulmonary Angioplasty in Patients With Chronic Thromboembolic Pulmonary Hypertension. Circ Cardiovasc Interv. 2018;11(12):e005884.
8. Ikeda N, Kubota S, Okazaki T, Iijima R, Hara H, Hiroi Y, et al. The predictors of complications in balloon pulmonary angioplasty for chronic thromboembolic pulmonary hypertension. Catheter Cardiovasc Interv. 2019;93(6):E349-E356.
9. Sznajder M, Dzikowska-Diduch O, Kurnicka K, Roik M, Wretowski D, Pruszczyk P, et al. Increased systemic arterial stiffness in patients with chronic thromboembolic pulmonary hypertension. Cardiol J. 2018 Sep 20. Doi.10.5603/CJ.a2018.0109
10. Ogawa A, Satoh T, Fukuda T, Sugimura K, Fukumoto Y, Emoto N, et al. Balloon Pulmonary Angioplasty for Chronic Thromboembolic Pulmonary Hypertension: Results of a Multicenter Registry. Circ Cardiovasc Qual Outcomes. 2017;10(11): pii: e004029.

Very Long Apneas during Prone Position in a Lean Patient with Coronary Artery Disease: Implications for the Cardiovascular Risk

Sofia Fontanello Furlan,[1] Viktor Sinkunas,[1] Pedro Rodrigues Genta,[1] Geraldo Lorenzi-Filho,[1] Luciano F. Drager[1]

Universidade de São Paulo Instituto do Coração,[1] São Paulo, SP – Brazil

Introduction

Obstructive sleep apnea (OSA) is a common condition characterized by recurrent upper airway obstructions during sleep, promoting intermittent hypoxia and sleep fragmentation.[1]Traditional risk factors for OSA include male gender and obesity. Overall, patients with severe OSA presented longer events and more severe hypoxemia. Supine sleep is consistently associated with more severe OSA rates in adults.[2] However, the relationship between OSA indices and prone position is inconsistent.[2] Here, we reported a very peculiar presentation of OSA characterized by very long respiratory events in a prone position in a lean female patient with a history of high blood pressure, diabetes mellitus, chronic kidney disease under dialysis therapy and a recent diagnosis of coronary artery disease (CAD).

Case Report

A 63 year-old female was electively admitted to the Hospital to perform a percutaneous coronary intervention (PCI) procedure. Eventhough she did not complain of daytime sleepiness (Epworth Sleepiness Scale: 9), her relatives described she was very sleepy, presented loud snoring and nocturnal breathing pauses during sleep. Upon inspection, there were no important signs of craniofacial changes that predisposed to OSA. Body-mass index (BMI) was within the normal range (25 kg/m^2) but arterial blood pressure was uncontrolled (152/84 mmHg). Interestingly, a recent ambulatory blood pressure monitoring (ABPM) showed a reverse systolic dipping pattern (blood pressure during sleep equal or higher than wakefulness) (Figure 1). She was under regular use of aspirin, carvedilol, amlodipine and atorvastatin. Arterial blood pressure medications were further adjusted by the medical team. The patient underwent a successful PCI in the *left anterior descending artery* using a bare metal stent. After the procedure, she underwent a sleep study using a portable monitor (Embletta Gold®). The patient had an apnea-hypopnea index of 26.7 events/hour with a lowest peripheral oxygen saturation (SpO_2) of 28% and a total time with a SpO_2 <90% of 33%. Very long apneas (19 episodes lasting >1 minute and the longest event lasting the incredible 3.21 minutes) (Figure 2) were observed. Of note, the patient spent 76% of the time in the prone position (her preferred sleep position).

The patient did not seek our outpatient sleep clinic despite we actively recommended treatment for OSA. After 11 months of the PCI, the patient suffered an acute myocardial infarction. Approximately 2 years after the PCI procedure, she suffered an episode of stroke and four months later a new fatal myocardial infarction during a nap at 3:00 pm despite using standard medications for CAD.

Discussion

This case called our attention due to the unusual presentation of OSA in a high cardiovascular risk patient: BMI in the normal range and very long respiratory events predominantly in the prone position. In a previous study, obstructive apneas lasting up to 3.89 min in a patient with autonomic dysfunction was reported, probably reflecting the lack of protective autonomic control in terminating the apneic events.[3] Our patient had no evidence of autonomic disease, despite the history of diabetes. Indeed, no periods of hypotension were observed in the ABPM. In contrast, we observed a reverse dipping pattern in the ABPM. Reverse dipping has been shown to be associated with a 4-fold increase in the probability of significant OSA, regardless the presence of sleep complaints or positive sleep questionnaires.[4]

One interesting finding is the unusual occurrence of obstructive events in the prone position. It is largely accepted that supine position predisposes to upper airway obstructions during sleep.[5] Preliminary studies reported prone position as adjunctive therapy for OSA.[6,7] In contrast, this case report underscore that prone position may not be an innocent bystander, as observed in infants.[8] Although no cause-effect relationship may be proven, it is conceivable that the prone position combined with a high arousal threshold may contribute to very long events observed during sleep in this patient.

Finally, it is worthy to mention that OSA patients with CAD had no benefits of continuous positive airway pressure (CPAP) in preventing cardiovascular disease according to the SAVE trial.[9] Severe hypoxia burden (as observed in this case) was not included in the usual SAVE study's profile, preventing any definitive conclusion on the benefits of OSA treatment among OSA patients with severe hypoxia burden. The lack of specific OSA treatment may have contributed to the observed cardiovascular outcomes.

Keywords

Angioplasty; Sleep Apnea Obstructive; Coronary Artery Disease; Percutaneous Coronary Intervention; Body Mass Index; Obesity; Blood Pressure Monitoring Ambulatory; Oxymetria.

Mailing Address: Sofia Fontanello Furlan •
Universidade de São Paulo Instituto do Coração - Av. Dr. Enéas de Carvalho Aguiar, 44. Postal Code 05403-000, São Paulo, SP – Brazil
E-mail: sofiaffurlan@yahoo.com.br, sofiaffurlan@gmail.com
Manuscript received March 10, 2020, revised manuscript June 10, 2020, accepted June 10, 2020

DOI: https://doi.org/10.36660/abc.20200191

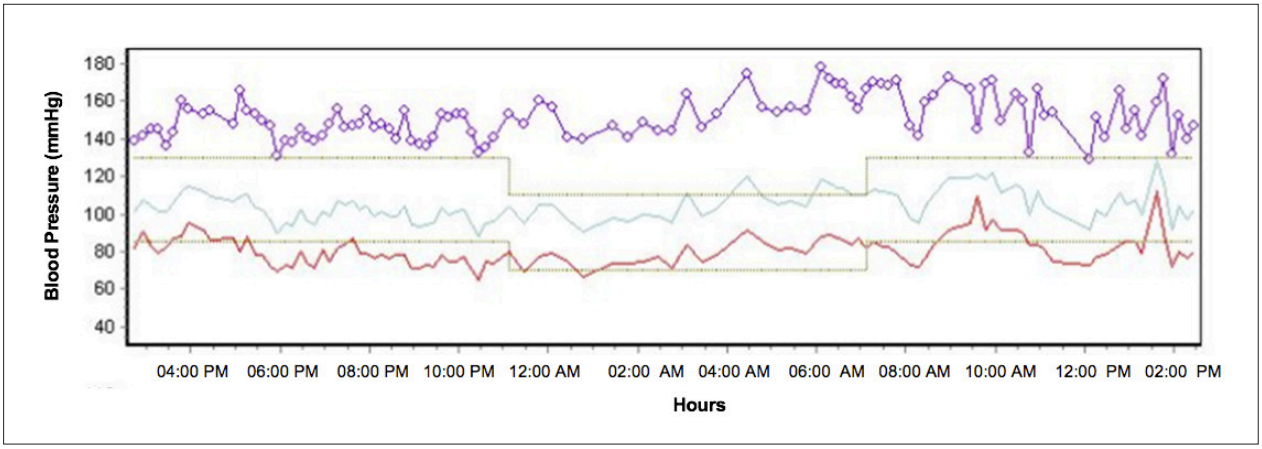

Figure 1 – *Ambulatory blood pressure monitoring showing reverse systolic blood pressure dipping pattern. Mean daytime blood pressure: 150x81 mmHg; Mean nighttime blood pressure: 155x79 mmHg.*

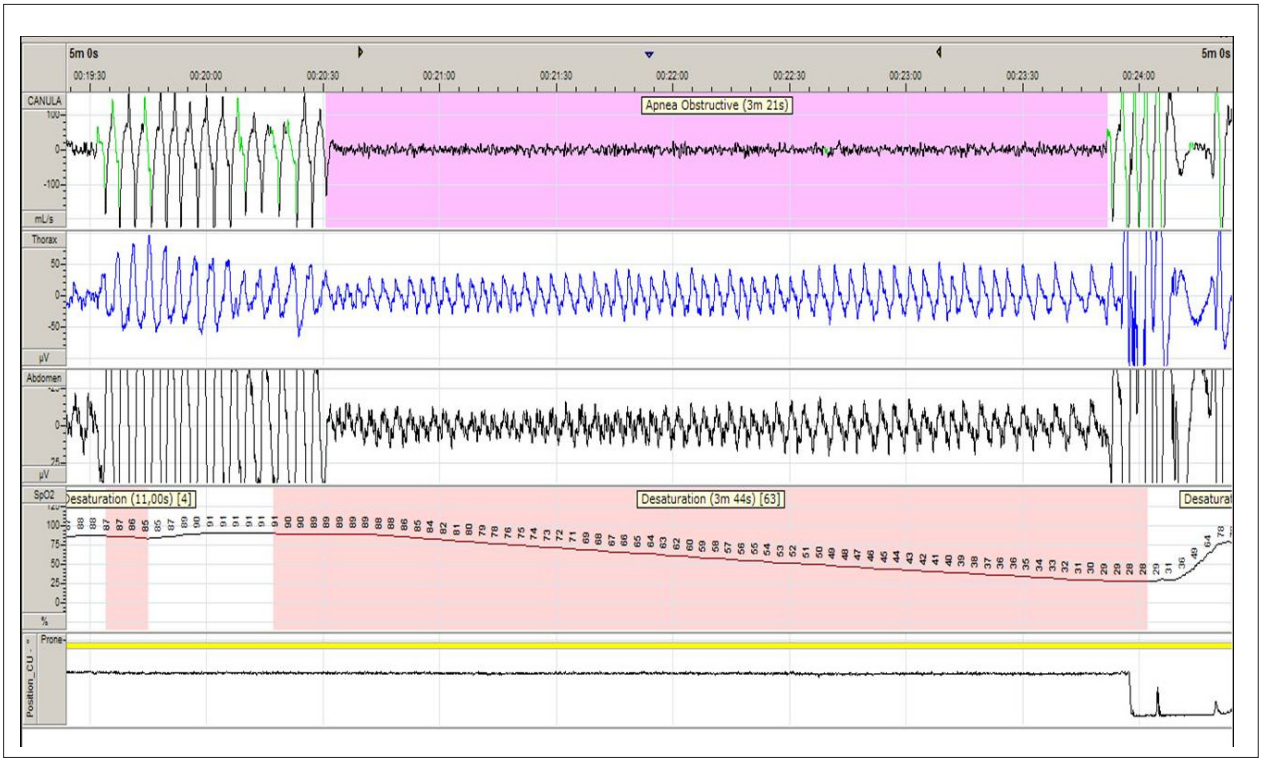

Figure 2 – *The longest obstructive apnea during sleep monitoring. Observe the severe related hypoxemia and the sensor position channel revealing prone position (yellow trace).*

Conclusion

This is an unusual case of very long apneas during prone position in a lean patient with CAD. As suggested in a multicenter observational study, the unfavorable follow-up suggests that OSA is not an innocent bystander in CAD, especially in the presence of diabetes.[10,11] Therefore, the neutral results of SAVE trial should not preclude treatment aiming potential cardiovascular benefits in high risk patients with severe hypoxemia.

Author Contributions

Conception and design of the research: Furlan SF, Drager L; Acquisition of data: Furlan SF, Sinkunas V; Analysis and interpretation of the data: Furlan SF, Sinkunas V, Drager L; Statistical analysis: Furlan SF; Obtaining financing: Lorenzi G, Drager L; Writing of the manuscript: Furlan SF, Sinkunas V, Genta PR, Lorenzi G, Drager L; Critical revision of the manuscript for intellectual content: Furlan SF, Genta PR, Drager L.

Potential Conflict of Interest

No potential conflict of interest relevant to this article was reported.

Sources of Funding

There were no external funding sources for this study.

Study Association

This study is not associated with any thesis or dissertation work.

Ethics approval and consent to participate

The patient participated in a previous study addressing the potential impact of sleep apnea after percutaneous coronary intervention (approved by the Ethics Committee of the Hospital das Clinicas da Universidade de São Paulo under the protocol number 3931/13/056). All the procedures in this study were in accordance with the 1975 Helsinki Declaration, updated in 2013. Informed consent was obtained from this patient.

References

1. Jordan AS, McSharry DG, Malhotra A. Adult obstructive sleep apnoea. Lancet. 2014;383(9918):736-47.
2. Menon A, Kumar M. Influence of body position on severity of obstructive sleep apnea: a systematic review. ISRN Otolaryngol. 2013:670381.
3. Aulakh PK, Westerman DE, Dedhia RC. The longest obstructive apnea you have ever seen: a patient with new-onset autonomic dysfunction. J Clin Sleep Med. 2018;14(5):893–5.
4. Genta-Pereira DC, Furlan SF, Omote DQ, Giorgi DM, Bortolloto LA, Lorenzi-Filho G, et al. Blood Pressure Patterns Predict Obstructive Sleep Apnea in Patients Undergoing Ambulatory Blood Pressure Monitoring. Hypertension. 2018; 72(4):979-985
5. Cartwright RD. Effect of sleep position on sleep apnea severity. Sleep 1984; 7(2):110–4
6. Afrashi A, Ucar ZZ. Effect of prone positioning in mild to moderate obstructive sleep apnea syndrome. Sleep Breath. 2015;19(3):1027-34.
7. Bidarian-Moniri A, Nilsson M, Rasmusson L, Attia J, Ejnell H. The effect of the prone sleeping position on obstructive sleep apnoea. Acta Otolaryngol. 2015;135(1):79-84.
8. Jeffery HE, Megevand A, Page HD. Why the prone position is a risk factor for sudden infant death syndrome. Pediatrics. 1999;104(2 Pt 1):263-9
9. McEvoy RD, Antic NA, Heeley E, Luo Y, Ou Q, Zhang X, et al. CPAP for prevention of cardiovascular events in obstructive sleep apnea. N Engl J Med. 2016; 375(10):919–31.
10. Lee CH, Sethi R, Li R, Ho HH, Hein T, Jim MH, et al. Obstructive Sleep Apnea and Cardiovascular Events After Percutaneous Coronary Intervention. Circulation. 2016;133(21):2008-17.
11. Koo CY, Drager LF, Sethi R, Ho HH, Hein T, Jim MH, et al. Sleep and Stent Study Investigators. Obstructive Sleep Apnea and Diabetes Independently Add to Cardiovascular Risk After Coronary Revascularization. Diabetes Care. 2018;41(2):e12-e14.

When Everything goes Wrong

Helder Santos,[1] Hugo Miranda,[1] Mariana Santos,[1] Inês Almeida,[1] Joaquim Peixoto,[2] Joana Chin,[1] Lurdes Almeida[1]

Departamento de Cardiologia, Centro Hospitalar Barreiro Montijo E.P.E.,[1] Barreiro - Portugal

Departamento de Medicina Interna, Centro Hospitalar Barreiro Montijo E.P.E.,[2] Barreiro - Portugal

Introduction

The Bentall procedure was described for the first time 50 years ago and has undergone several improvements through the years. This technique is considered to be a longstanding and safe procedure. However, as any surgery, it can have several complications such as anastomotic pseudoaneurism, myocardial infarction and endocarditis.[1]

In developed countries with differentiated access to health care and prophylaxis, endocarditis is an uncommon pathology, associated to frequent complications and high mortality rates. Antibiotic therapy aims to eradicate the responsible microorganism.[2] However, some of the drugs used cause several side effects, like the DRESS (Drug Reaction with Eosinophilia and Systemic Symptoms) syndrome.

The DRESS syndrome was firstly described by Bocquet et. al. in 1996, in patients with constitutional symptoms, lymphadenopathy and peripheral eosinophilia. It is considered a severe idiosyncratic and hypersensitivity reaction to drugs, with extensive clinical features. Its incidence is unknown, but it occurs more frequently in adults.[3,4] Several drugs were associated to DRESS, yet vancomycin is one of the most frequent ones.[3,5] DRESS has a broad spectrum of clinical conditions, ranging from mild symptoms to multiple-organ failure. However, drug exposing time, individual susceptibility and prompt diagnosis can influence the patient's response. Mortality rates range from 3 to 10% and prompt diagnosis and drug withdrawal is important to achieve a favorable outcome.[3,4]

The authors present a unique case that reflects a set of sporadic events that occurred in one patient.

Case Report

The patient is a 60-year-old male with past medical history of arterial hypertension, dyslipidemia and Bentall procedure 8 months prior to admission, with implantation of a St. Jude mechanical aortic valve and aortic Uni-Graft 28 mm due to ascending aortic aneurysm (56 mm).

At the emergency room, the patient presented dyspnea, fatigue, weariness and sweating. Physical examination revealed heart rate of 120 bpm, blood pressure of 170/94 mmHg, pulmonary rales and peripheral edema. Blood tests revealed anemia and elevated biomarkers of myocardial necrosis. Electrocardiogram (EKG) showed sinus rhythm, right bundle branch block, T wave inversion of 0.05 mV in DI and aVL, and ST depression of 0.1 mV from V4 to V6. Transthoracic echocardiography revealed normal mechanical aortic valve function with mild prosthetic leak and preserved left ventricular function. The patient presented recurrent acute pulmonary edema episodes during the hospital stay. In one of these episodes, dynamic EKG abnormalities and a new rise of cardiac biomarkers were identified. The patient progressed into cardiogenic shock with new left ventricular systolic dysfunction and diffuse hypokinesia. Coronary angiography ruled out coronary artery disease and, nonetheless, revealed an extrinsic compression of left coronary artery, suggesting pseudoaneurysm between the Uni-Graft and the mechanical aortic valve that compressed the left coronary artery. This finding was confirmed in a cardiac computed tomography angiography (Figure 1).

The patient was submitted to pseudoaneurysm resection and aortic mechanical valve replacement. During the surgery, images of vegetation suggesting infectious endocarditis was identified. Empiric treatment with flucloxacillin, vancomycin, ceftriaxone and rifampicin were started, with negative blood culture tests and initial favorable response.

At the 24th day of antibiotic therapy, the patient presented sudden fever associated with non-confluent, non-pruritic maculopapular rash on the abdomen, upper and lower limbs and thorax, as well as lymphadenopathies. Initially, rifampicin toxicity was admitted, and the drug was suspended with gradual clinical recovery.

Nevertheless, 12 days later, the patient presented a similar clinical condition with rash (Figures 2 and 3), fever, lymphocytosis with nuclear dysmorphia, eosinophilia, acute hepatitis, acute kidney injury and altered states of consciousness (fluctuating periods of mental confusion and obnubilation). Deterioration of clinical course rapidly occurred, requiring invasive ventilation and vasopressor support. Cranial, thoracic and abdominal computed tomography showed no pathological findings. Transthoracic echocardiogram was repeated and prosthetic valve function was normal. Lumbar puncture exhibited normal results. Blood cultures, mechanical valve culture, serological tests (except for herpes zoster) and autoimmunity tests were negative. Skin biopsy revealed inflammatory reaction. After ruling out further pathologies through an exhaustive work-up, the hypothesis of DRESS syndrome secondary to vancomycin was assumed.

Vancomycin withdrawal along with intensive care support and high-doses of corticotherapy led to gradual improvement of the patient organ's function. At 1 year of follow-up, no complications or deficits were found.

Keywords

Acute Coronary Syndrome; Aortic Valve,Diseases; Endocarditis; Antibiotic Prophylaxis; Drug Hypersensibility Syndrome; Postoperative Complications.

Mailing Address: Helder Santos •
Departamento de Cardiologia, Centro Hospitalar Barreiro-Montijo - Avenida Movimento das Forças Armadas, 2834-003. Barreiro - Portugal
E-mail: helder33689@gmail.com
Manuscript received December 25, 2019, revised manuscript April 27, 2020, accepted June 10, 2020

DOI: https://doi.org/10.36660/abc.20190907

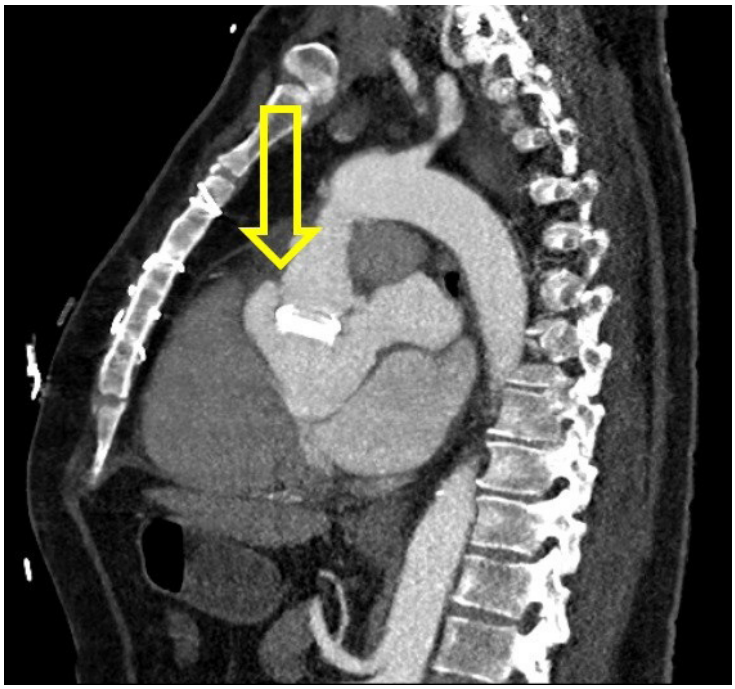

Figure 1 – *Cardiac computed tomography angiography showed extrinsic compression of the left coronary artery secondary to pseudoaneurysm between the Uni-Graft and mechanical aortic valve.*

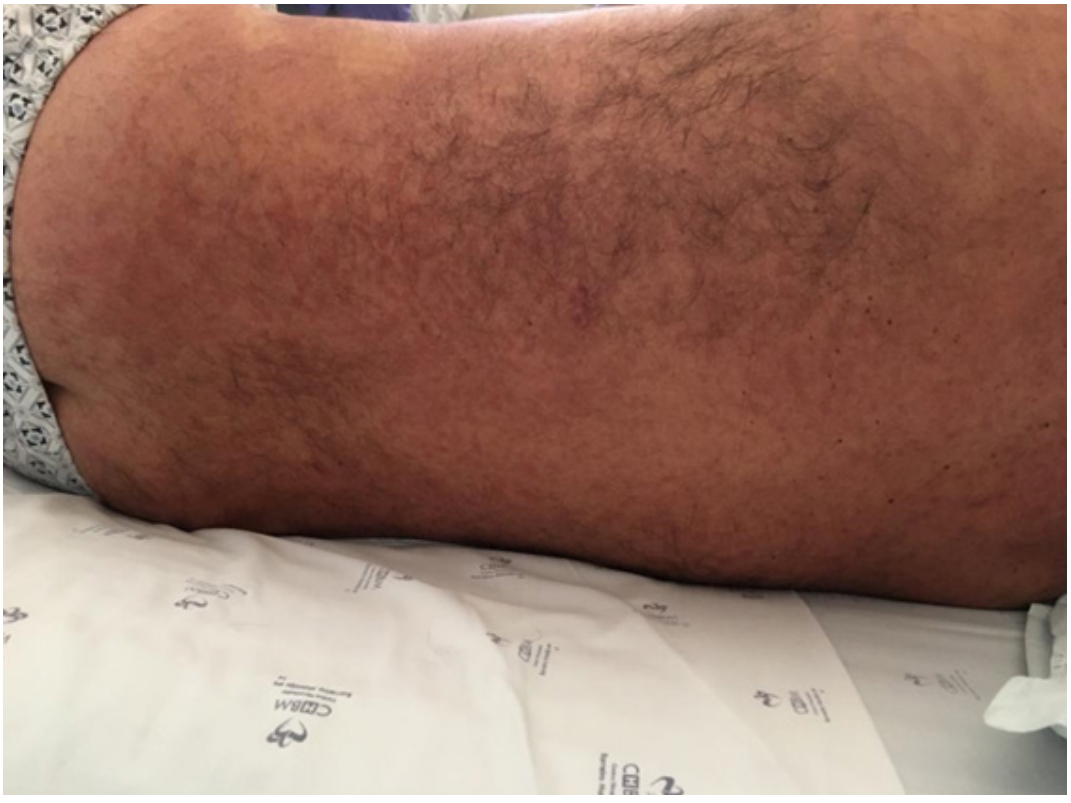

Figure 2 – *Non-confluent, non-pruritic maculopapular rash on the thorax and back.*

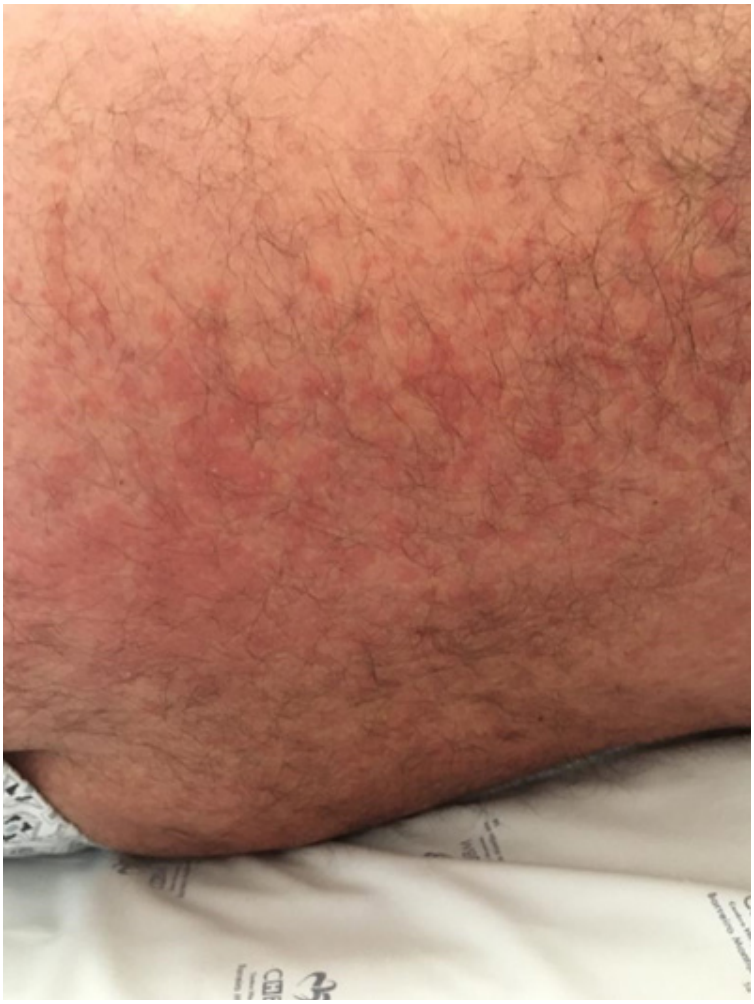

Figure 3 – *Non-confluent, non-pruritic maculopapular rash on the back.*

Discussion

Technical problems on Bentall procedure can promote dehiscence, which may lead to anastomotic pseudoaneurysm. The dehiscence site and the surrounding structures may lead to cardiovascular events.[1,6]

Developed countries have relevant incidence of prosthetic valve endocarditis and blood cultures are the gold standard for the diagnosis.[2] The modified Duke criteria provide a standardized diagnosis and should be carefully applied in infective endocarditis. As for prosthetic valve endocarditis, the modified Duke criteria have lower diagnostic accuracy. The case reported presented two minor criteria, fever and previous heart surgery. According to the Duke criteria, three minor criteria are required for a possible endocarditis.[2] Nevertheless, we chose to assume that the diagnosis and empiric treatment was started, even in the presence of negative cultures of the resected valvular tissue.

Pathogeny of the DRESS syndrome is poorly known. However, an interaction is globally accepted between different mechanisms, such as patient's genetic predispositions, metabolic abnormalities leading to accumulation of drug metabolites and drug-virus interactions leading to the reactivation of human herpes virus (HHV) 6 and 7. Clinical manifestations appear after a long period of drug exposure and consist in skin rashes, hematological abnormalities, lymphadenopathies and multisystemic dysfunction.[3] If DRESS is suspected, an HHV test is recommended, since HHV infection is related to higher complications and longer hospitalization stay.[7]

The RegiSCAR project (European Registry of Severe Cutaneous Adverse Reactions to drugs and collection of biological samples) suggests that at least three of the following criteria are required for diagnosis: hospitalization, fever, suspected reaction to drugs, acute rash, lymphadenopathies in 2 different areas, organ dysfunction and blood abnormalities.[8] According to the SCAR-J (Japanese group of severe cutaneous adverse reactions to drugs),[9] diagnosis is established by the presence of the 5 following criteria: maculopapular rash after 3 weeks of treatment, fever, lymphadenopathies, leukocytosis, hepatitis and HHV 6 reactivation. Therefore, our patient exhibited 6 RegiSCAR criteria for DRESS diagnosis. Yet, using

the SCAR-J criteria, our patient does not meet all requirements for DRESS diagnosis, since HHV 6 reactivation was not detected, being classified as an atypical DRESS presentation.

Current recommendations to guide the treatment for the DRESS syndrome are based on case reports and expert opinions, and all of them recommend the immediate suspension of the responsible drug and, if possible, reduction of other drugs. Additionally, corticotherapy is usually used. However, there are no studies revealing any clear efficacy and some authors advocate that it can exacerbate viral reactivation. DRESS patients should have long-term follow-up because they have higher risk of autoimmune diseases.[10]

Endocarditis is a frequent complication in patients submitted to cardiac surgery. The use of vancomycin has increased over the last years and therefore it is more frequently associated with the DRESS syndrome. Since clinical manifestations and laboratory abnormalities are unspecific, the DRESS diagnosis relies on an early clinical suspicion. Prompt recognition and identification of the DRESS syndrome is essential to an effective therapeutic approach and low mortality rates.

Acknowledgements

The authors thank to every health professionals in Centro Hospitalar Barreiro-Montijo E. P. E. for the contribution to this report.

Author Contributions

Conception and design of the research, Analysis and interpretation of the data and Critical revision of the manuscript for intellectual content: Santos H, Miranda H, Santos M, Almeida I, Chin J, Almeida L; Acquisition of data: Santos H, Miranda H, Santos M, Chin J; Statistical analysis: Santos H, Santos M; Writing of the manuscript: Santos H, Miranda H, Santos M, Almeida I, Chin J.

Potential Conflict of Interest

No potential conflict of interest relevant to this article was reported.

Sources of Funding

There were no external funding sources for this study.

Study Association

This study is not associated with any thesis or dissertation work.

Ethics Approval and Consent to Participate

This article does not contain any studies with human participants or animals performed by any of the authors.

References

1. Sioris T, David TE, Ivanov J, Armstrong S, Feindel CM. Clinical outcomes after separate and composite replacement of the aortic valve and ascending aorta. J Thorac Cardiovasc Surg.2004;128(2):260-5.
2. Habib G, Lancellotti P, Antunes MJ, Bongiorni MG, Casalta J-P, Del Zotti F, et al. 2015 ESC guidelines for the management of infective endocarditis: the task force for the management of infective endocarditis of the European Society of Cardiology (ESC) endorsed by: European Association for Cardio-Thoracic Surgery (EACTS), the European Association of Nuclear Medicine (EANM). Eur Heart J. 2015;36(44):3075-128.
3. Cacoub P, Musette P, Descamps V, Meyer O, Speirs C, Finzi L, et al. The DRESS syndrome: a literature review. Am J Med. 2011;124(7):588-97.
4. Husain Z, Reddy BY, Schwartz RA. DRESS syndrome: Part I. Clinical perspectives. J Am Acad Dermatol. 2013;68(5):693. e1- e14.
5. Kardaun S, Sekula P, Valeyrie-Allanore L, Liss Y, Chu C, Creamer D, et al. Drug reaction with eosinophilia and systemic symptoms (DRESS): an original multisystem adverse drug reaction. Results from the prospective RegiSCAR study. Br J Dermatol. 2013;169(5):1071-80.
6. Haddy SM. Aortic pseudoaneurysm after Bentall procedure. JCardiothorac Vasc Anesth. 1999;13(2):203-6.
7. Tohyama M, Hashimoto K, Yasukawa M, Kimura H, Horikawa T, Nakajima K, et al. Association of human herpesvirus 6 reactivation with the flaring and severity of drug-induced hypersensitivity syndrome. Br J Dermatol. 2007;157(5):934-40.
8. Kardaun S, Sidoroff A, Valeyrie-Allanore L, Halevy S, Davidovici B, Mockenhaupt M, et al. Variability in the clinical pattern of cutaneous side-effects of drugs with systemic symptoms: does a DRESS syndrome really exist? BrJ Dermatol. 2007;156(3):609-11.
9. Shiohara T, Iijima M, Ikezawa Z, Hashimoto K. The diagnosis of a DRESS syndrome has been sufficiently established on the basis of typical clinical features and viral reactivations. Br J Dermatol. 2007;156(5):1083-4.
10. Chen Y-C, Chang C-Y, Cho Y-T, Chiu H-C, Chu C-Y. Long-term sequelae of drug reaction with eosinophilia and systemic symptoms: a retrospective cohort study from Taiwan. J Am Acad Dermatol. 2013;68(3):459-65.

Isolated Right Ventricle Myocardial Infarction - Is the Right Ventricle Still the Forgotten Ventricle?

Ana Marques,[1] *Inês Cruz,*[1] *Alexandra Briosa,*[1] *Isabel João,*[1] *Sofia Almeida,*[1] *Hélder Pereira*[1]

Departamento de Cardiologia, Hospital Garcia de Orta,[1] *Almada - Portugal*

Introduction

Isolated right ventricular myocardial infarction is extremely rare, and it is often silent, with only 25% of patients developing clinically evident hemodynamic manifestations on presentation.[1] Current management of acute myocardial infarction is based on prompt diagnosis and immediate revascularization.[2] About 90% of patients presenting with ST-segment elevation myocardial infarction have an explanatory coronary artery stenosis or occlusion.[3] Myocardial infarction with non-obstructive coronary arteries (MINOCA) should lead the treating physician to investigate underlying causes, since failure to identify the underlying cause may result in inadequate and inappropriate therapy in these patients.

We describe a case of isolated right ventricular myocardial infarction with normal physical examination, transthoracic echocardiograms, and non-obstructive coronary artery disease on coronary angiography, whose definitive diagnosis was established by cardiac magnetic resonance imaging.

Case Report

A 64-year-old white male was admitted to the hospital with a 1-hour history of sudden-onset acute oppressive anterior chest pain without other associated symptoms. After sublingual nitrate therapy, the patient presented total pain relief. His medical history included arterial hypertension, dyslipidemia, and former smoking.

At admission, the patient was conscious and hemodynamically stable (blood pressure: 130/70 mmHg and heart rate: 70 bpm), with apyrexy, eupnea, and peripheral oxygen saturation of 99%. No changes in cardiac and pulmonary auscultation were noted, and there was no elevated jugular venous pressure or edemas of lower extremities. Abdominal inspection was also normal.

Electrocardiography showed sinus rhythm and heart rate of 96 bpm, with ST-segment elevation in both inferior and right leads as well as ST-segment depression with T-wave inversion in lead aVL (Figure 1, panel A). Dual antiplatelet and anticoagulation therapy was started. Immediate invasive coronary angiography was performed, revealing a non-obstructive 40% to 50% lesion of the proximal right coronary artery, with TIMI grade flow 3 (Figure 1, panel B).

The transthoracic echocardiogram at admission did not reveal significant changes such as segmental wall motion abnormalities, valvopathies, pericardial effusion, or signs of aortic dissection. Both left and right ventricles were non-dilated, and they had preserved ventricular systolic function (TAPSE 20 mm, tricuspid annular systolic velocity 12.7 cm/s, and left ventricular ejection fraction 65%, with the biplane Simpson method). Both right and left atria were non-dilated (Supplementary Material).

During hospitalization, the patient remained asymptomatic without recurrence of chest pain, heart failure symptoms, or arrhythmias documented by continuous electrocardiographic monitoring.

Laboratory analysis showed elevated high-sensitivity troponin T levels (maximum value 1,790 ng/L, normal value < 13 ng/L). The remaining laboratory analyses were within the normal ranges (NT-proBNP: 97 ng/L, D-dimer: 0.3 mg/L, hemoglobin: 14.1 g/L, leucocytes: 5,700, C-reactive protein: 0.2 mg/dL, creatinine: 0.9 mg/dL, AST: 71 UI/L, ALT: 35 UI/L, GGT: 49 UI/L, total bilirubin: 0.6 mg/dL, TSH 2.1: mU/L, and free T4: 1.22 mU/L).

The electrocardiography performed 2 days after admission showed resolution of the abnormalities noted at admission. An isolated Q wave was observed in lead DIII (Supplementary Material). The transthoracic echocardiography performed 2 days after admission did not show any abnormalities, such as wall motion abnormalities or dysfunction of the right ventricle.

Due to the presence of MINOCA, cardiac magnetic resonance imaging was performed 4 days after admission. The cardiac magnetic resonance imaging showed hypokinesis of the right ventricle inferior wall, with myocardial edema on T2-weighted images and myocardial necrosis on late gadolinium enhancement analysis (Figure 2). Final diagnosis of isolated right ventricular myocardial infarction was established.

Discussion

The early recognition of right ventricle myocardial infarction in patients with acute myocardial infarction is of prime importance, not only for prognostic purposes, but also because it can guide specific therapy, including aggressive primary percutaneous coronary intervention, and avoid treatments that would further lower right ventricular preload (nitrates and diuretics), thus compromising the patient's condition.[4,5]

The diagnosis of this entity is commonly made from physical examination, electrocardiography, echocardiography, and hemodynamic measurements.[5]

Keywords

Myocardial Infarction; Coronary Artery Disease; Myocardial Revascularization; Percutaneous Coronary Intervention; Diagnosis Imaging.

Mailing Address: Ana Marques •
Avenida Torrado da Silva, 2805-267, Almada - Portugal
E-mail: ana.smc.25@gmail.com
Manuscript received February 28, 2020, revised manuscript May 23, 2020, accepted June 16, 2020

DOI: https://doi.org/10.36660/abc.20200164

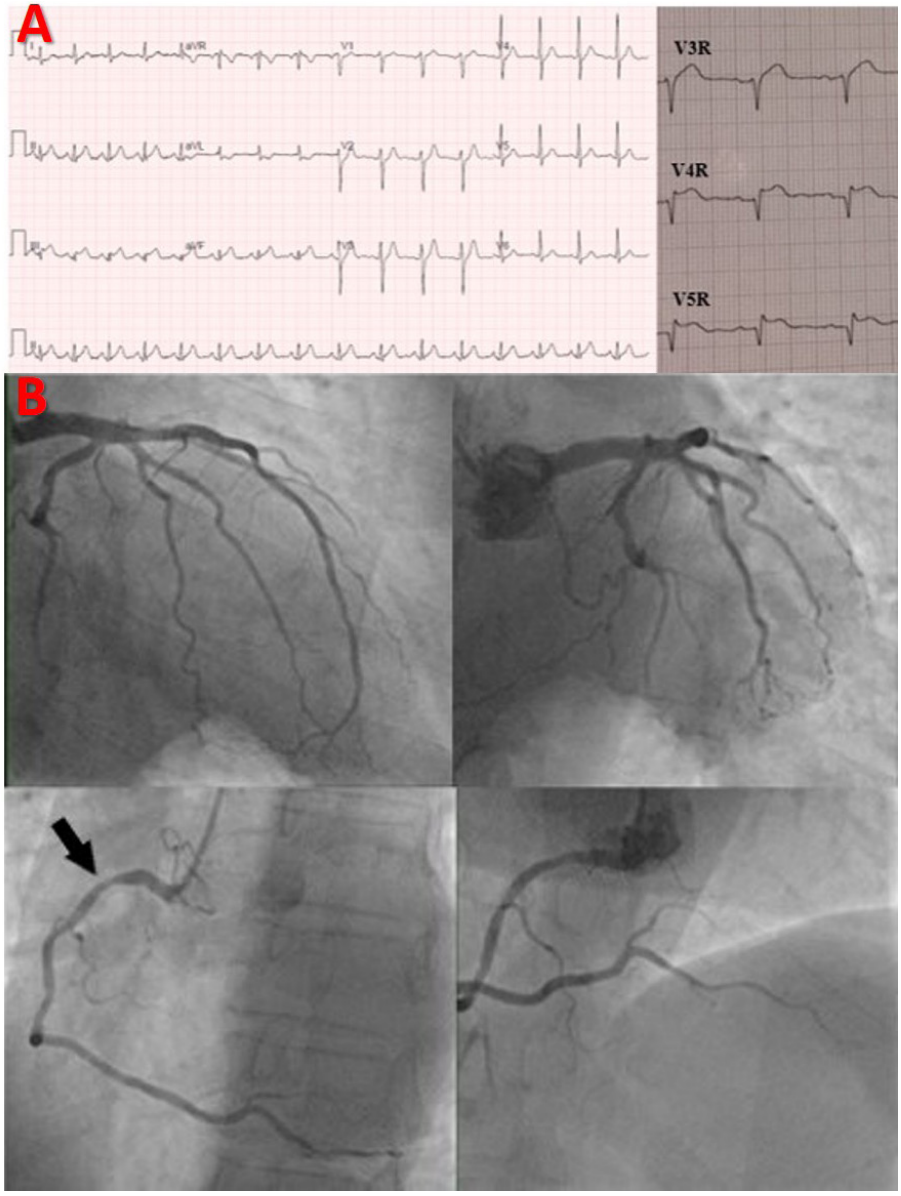

Figure 1 – *Panel A: Electrocardiography at admission showing ST-segment elevation in both inferior and right leads and ST-segment depression with T-wave inversion in lead aVL. Panel B: Coronary angiography showing a non-obstructive 40% to 50% lesion of the proximal right coronary artery (arrow), with TIMI grade flow 3.*

The classic triad observed during physical examination consists of hypotension, clear lung fields, and elevated jugular venous pressure.[6]

Right ventricle myocardial infarction should be suspected in cases of infero-posterior myocardial infarction, and right precordial lead electrocardiogram should be performed, since right ventricular ischemia occurs in up to half of cases of inferior myocardial infarction.[4,5]

Echocardiography can depict abnormal movement of the right ventricular free wall, and it can assess the presence of right ventricular dysfunction or dilation.[6] Additional features of right ventricular involvement include paradoxical motion of the septum (interventricular and interatrial) and the presence of right atrial enlargement or tricuspid regurgitation.[6]

Cardiac magnetic resonance imaging can be useful for diagnosis, because it is more sensitive than electrocardiography and echocardiography.[7]

Coronary angiography usually leads to the final diagnosis.[8] Right ventricle myocardial infarction occurs mainly due to occlusion of the right coronary artery proximal to the major right ventricular branches in the context of inferior myocardial infarction.[9] It may also occur due to occlusion of the left circumflex artery in patients with left-dominant circulation and, less commonly, in anterior infarctions, as the anterior

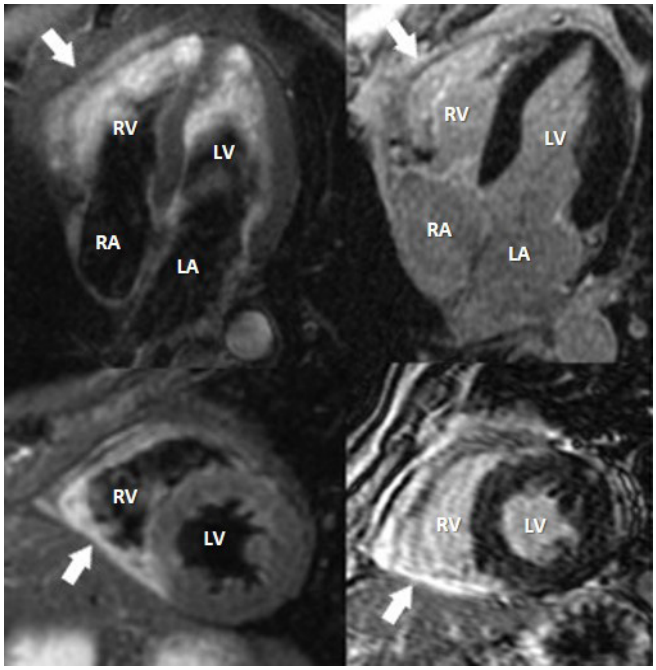

Figure 2 – *Diagnosis of isolated acute right ventricular myocardial infarction by cardiac magnetic resonance imaging. On the T2-weighted images (left panel), increased signal intensity in the right ventricular inferior wall was detected, indicating myocardial edema (arrows). On late gadolinium enhancement (LGE) analysis (right panel), LGE was seen in the right ventricular inferior wall (arrows), indicating the presence myocardial necrosis. LA: left atrium; LV: left ventricle; RA: right atrium; RV: right ventricle.*

part of the right ventricular free wall is supplied by collaterals from the left anterior descending artery.[10]

Our case of isolated right ventricle myocardial infarction illustrates an uncommon cause of myocardial infarction. Not only was it unique in being a rare pathology, but it was also a diagnostic challenge. Physical examination, echocardiography, and coronary angiography were not able to establish the final diagnosis, given that they did not show significant abnormalities. This case highlights the importance of electrocardiography and the essential role of cardiac magnetic resonance in the differential diagnosis of patients with MINOCA; establishing correct definitive diagnosis is of the utmost importance in order to provide appropriate therapy, and it can help to anticipate and prevent complications that differ according to the etiology.

Author contributions

Data acquisition: Marques A, Cruz I, Briosa A, Almeida S; Writing of the manuscript: Marques A; Critical revision of the manuscript for intellectual content: Cruz I, João I, Pereira H.

Potential Conflict of Interest

No potential conflict of interest relevant to this article was reported.

Sources of Funding

There were no external funding sources for this study.

Study Association

This study is not associated with any thesis or dissertation work.

Ethics approval and consent to participate

This article does not contain any studies with human participants or animals performed by any of the authors.

References

1. Shah PK, Maddahi J, Berman DS, Pichler M, Swan HJC. Scintigraphically detected predominant right ventricular dysfunction in acute myocardial infarction: clinical and hemodynamic correlates and implications for therapy and prognosis. J Am Coll Cardiol. 1985;6(6):1264–72.
2. Ibanez B, James S, Agewall S, Antunes MJ, Bucciarelli-Ducci C, Bueno H, et al. 2017 ESC Guidelines for the management of acute myocardial infarction in patients presenting with ST-segment elevation. Eur Heart J. 2018;39(2):119–77.
3. Dewood MA, Spores J, Notske R, Mouser LT, Burroughs R, Golden MS, et al. Prevalence of Total Coronary Occlusion during the Early Hours of Transmural Myocardial Infarction. N Engl J Med. 1980;303(16):897–902.
4. Namana V, Gupta SS, Abbasi AA, Raheja H, Shani J, Hollander GV.-S pd. Right ventricular infarction. Cardiovasc Revasc Med. 2018;19(1):43–50.
5. Kakouros N, Cokkinos D V. Right ventricular myocardial infarction: Pathophysiology, diagnosis, and management. Postgrad Med J. 2010;86(1022):719–28.
6. Ondrus T, Kanovsky J, Novotny T, Andrsova I, Spinar J, Kala P. Right ventricular myocardial infarction: From pathophysiology to prognosis. Exp Clin Cardiol. 2013;18(1):27–30.
7. Kumar A, Abdel-Aty H, Kriedemann I, Schulz-Menger J, Gross CM, Dietz R, et al. Contrast-Enhanced Cardiovascular Magnetic Resonance Imaging of Right Ventricular Infarction. J Am Coll Cardiol. 2006;48(10):1969–76.
8. Palfy JA, Tomás M, Farré J, Navas MA, Navarro F, Orejas M, et al. Pure right ventricular infarction resulting from coronary ectasia: Importance of diagnostic imaging. Circ J. 2002;66(2):213–5.
9. Bowers TR, O´Neill WW, Pica M, Goldstein JA. Patterns of coronary compromise resulting in acute right ventricular ischemic dysfunction. Circulation. 2002;106(9):1104–9.
10. Farrer-Brown G. Vascular pattern of myocardium of right ventricle of human heart. Br Heart J. 1968;30(5):679–86.

*Supplemental Materials

For additional information, please click here.

Three-dimensional Echocardiography Reveals the True Enemy in a Young Male with ST-Elevation Myocardial Infarction and Severe Mitral Regurgitation: Posterior Mitral Valve "Pseudo-Cleft" and Prolapse

Sorina Mihaila,[1] Andreea Elena Velcea,[1] Luigi Paolo Badano,[2,3] Vinereanu Dragos,[1] Denisa Muraru[2,3]

University of Medicine and Pharmacy Carol Davila Bucharest - Emergency University Hospital Bucharest,[1] Bucharest - Romania
Istituto Auxologico Italiano, IRCCS, Department of cardiac, neural and metabolic sciences, San Luca Hospital,[2] Milan - Italy
University of Milano-Bicocca, Department of Medicine and Surgery,[3] Milan - Italy

Introduction

Three-dimensional echocardiography (3DE) plays an increasingly important role in the diagnosis of valvular heart disease, in the assessment of valvular morphology in an anatomical manner, and in establishing valve repairability, beyond the limitations of conventional two-dimensional echocardiography (2DE).[1]

We report the case of a young patient presenting with acute anterior ST-segment elevation myocardial infarction and severe mitral regurgitation (MR) after successful primary percutaneous coronary intervention (PCI) of the left anterior descending artery, whose three-dimensional transesophageal echocardiography (3D TEE) revealed an unexpected cause of the MR, namely, complex mitral valve (MV) pathology consisting of prolapse of the P_{2-3} scallops, flail chordae, and pseudo-cleft of the posterior leaflet separating the P_1 from the P_2 segment.

Case Report

A 38-year-old male patient, without any known cardiovascular risk factors, presented with acute onset of constrictive thoracic pain. Cardiac examination revealed regular rhythm, apical systolic murmur, and normal blood pressure. Emergency 12-lead resting electrocardiogram showed ST-segment elevation in the V_{1-6} leads and recurrent non-sustained ventricular tachycardia. The emergency coronary angiogram showed acute thrombotic occlusion of the proximal left anterior descending artery, non-critical stenosis of the right coronary artery, and 90% stenosis of the left circumflex artery. Primary PCI with stenting of the left anterior descending artery was performed, with good procedural results.

Keywords

Mitral Valve/abnormalities; Myocardial Infarction; Echocardiography, Three Dimensional/methods; Diagnosis Imaging; Young Adult.

Mailing Address: Sorina Mihaila Baldea •
Splaiul Independentei no 169, sector 5, 10th floor, Bucharest, Romania - Cardiology and Cardiovascular Surgery Department University Hospital of Bucharest, Romania. CEP 050098
Email: sorinamihaila1981@gmail.com
Manuscript received July 23, 2019, revised manuscript June 11, 2020, accepted August 05, 2020

DOI: https://doi.org/10.36660/abc.20190485

Post-procedural transthoracic 2DE showed non-dilated left ventricle (LV), septal wall motion abnormalities, and mild LV systolic dysfunction (LV ejection fraction = 50%), as well as moderate dilation of the left atrium (LA) and severe MR with an eccentric jet, directed anteriorly into the LA (holosystolic regurgitation, effective regurgitant orifice area = 0.4 cm^2, regurgitant volume = 55 ml/m^2). A mild prolapse of the posterior MV leaflet was also detected by two-dimensional transthoracic echocardiography (2D TTE). However, neither the septal wall motion abnormality nor the MV prolapse as seen by 2D TTE entirely explained the severity of the MR. In this context, the mechanisms and the severity of the MR were further explored using transesophageal echocardiography, including 3DE assessment. 3D TEE assessment of the MV from the "surgical view" showed prolapse of the P_{2-3} segments (Figure 1, Panel A), a ruptured chordae attached to the posterior MV leaflet, and a deep indentation of the posterior MV (Figure 1, Panel B), leading to an eccentric regurgitant jet into the LA up to the pulmonary veins. To establish MV repairability, the exam was completed with 3DE assessment of the MV from the ventricular view (Figure 1, Panel C), where a pseudo-cleft of the posterior leaflet was detected, with the P_1 scallop separated from the P_{2-3} prolapsing segments. Color 2D TEE showed a "split" jet of MR (Figure 2, Panel A), while color 3D TEE showed an eccentric MR jet, with wide origin, directed anteriorly (Figure 2, Panel B and Panel C), further explaining the mechanism of the MR.

Potential acquired causes of these morphological findings, such as previous MV trauma, surgery, or infective endocarditis were excluded, and the final diagnosis was severe MR due to complex MV prolapse of the P_{2-3} segments and ruptured chordae attached to the posterior MV leaflet, associated with a pseudo-cleft of the posterior leaflet between the P_1 and P_2 segments. The patient was further referred for surgical opinion, due to enlargement of the LA (showing a prolonged evolution of the MR), and new onset of symptoms after the acute event (exercise dyspnea). MV repair, including prolapse resection, suture of the MV pseudo-cleft, and mitral annuloplasty were successfully performed, associated with grafting of the left circumflex artery. At three-year follow-up, the patient showed no recurrence of the MR.

Discussion

Our clinical case shows the usefulness of 3DE for the diagnosis and morphological assessment of complex MV lesions, especially when the etiology is uncertain, as well as its role in planning surgical procedures. Initial suspicion of

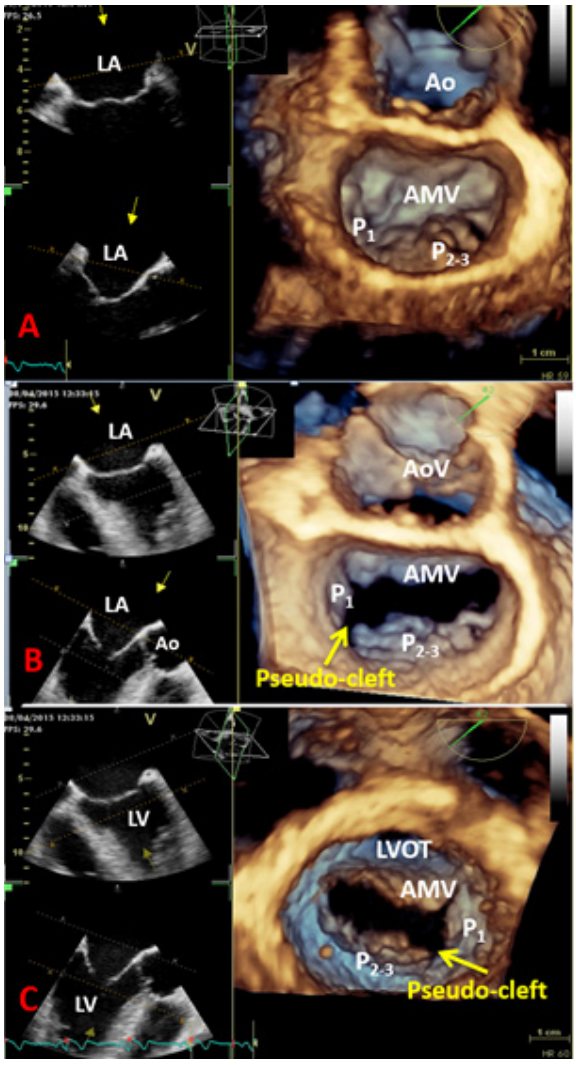

Figure 1 – *Three-dimensional morphological assessment of the mitral valve (transesophageal approach). Panel A. "Surgical view" of the closed mitral valve, seen from the left atrial side, which shows a complex prolapse of the P2-3 scallops. The anterior mitral valve leaflet shows normal morphology. Panel B. Opening of the mitral valve reveals that the P1 segment is separated from the P2-3 segments, raising the suspicion of a pseudo-cleft. Panel C. The mitral valve visualized from the left ventricular side. The pseudo-cleft of the posterior mitral valve leaflet, between the P1 and the P2-3 segments, can be identified. AMV: anterior mitral valve; Ao: aorta; AoV: aortic valve; LA: left atrium; LV: left ventricle; LVOT: left ventricular outflow tract.*

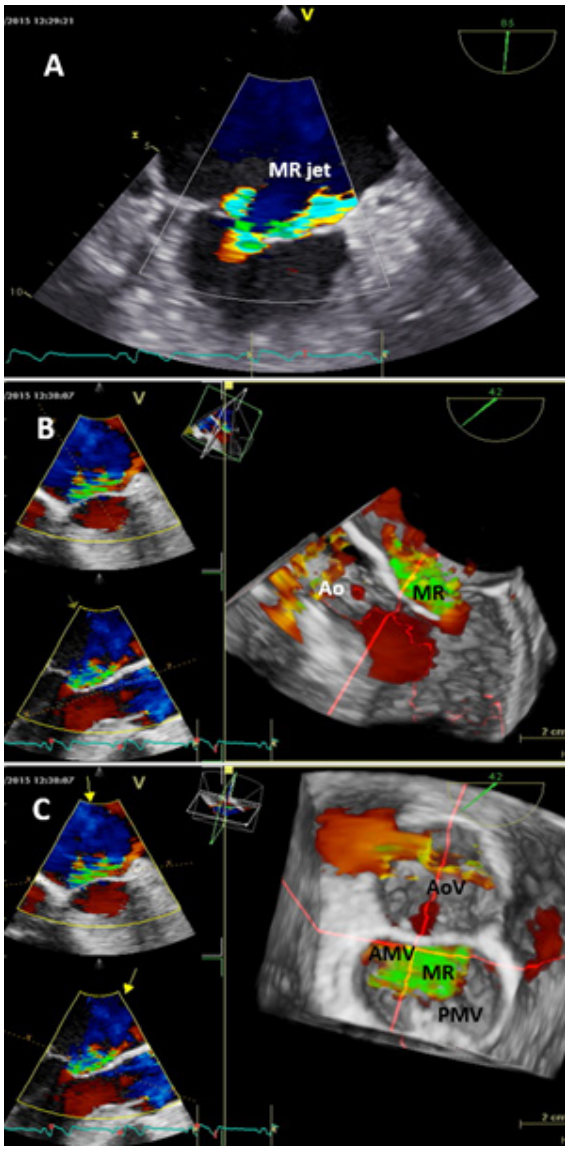

Figure 2 – *Two- and three-dimensional color assessment of the mitral regurgitation (transesophageal approach). Panel A. The mitral valve, visualized at 85 degrees, shows the two components of the mitral regurgitation, caused by the prolapse and the pseudo-cleft. Panel B. Long-axis view throughout the A2/P2 scallops shows the mitral regurgitation jet caused by the prolapse of P2, opposite the scallop. Panel C. The "surgical view" of the mitral valve shows the wide origin of the mitral regurgitation jet, seen from the left atrium, which is directed anteriorily (only retrograde flows are displayed). AMV: anterior mitral valve, Ao: aorta, AoV: aortic valve, MR: mitral regurgitation, PMV: posterior mitral valve.*

the MR etiology was ischemic; however, the short period of ischemia (less than 2 hours until revascularization), minor LV wall motion abnormalities, and good LV systolic function rendered this cause improbable. The careful 2DE assessment revealed mild prolapse of the posterior MV, which was also insufficient to explain the severity of the MR. Conversely, 3D TEE revealed complex MV prolapse of the P_{2-3} segments, a ruptured chordae, and pseudo-cleft of the posterior MV leaflet separating the P_1 from the P_2 scallop.

Clefts are hypothesized to be a result of incomplete expression of an endocardial cushion defect, most often involving the middle part of the anterior MV leaflet.[2,3] True clefts affecting the posterior MV are extremely rare.[2] However, pseudo-clefts are a separate class of morphologic anomalies of the posterior MV leaflet. Pseudo-clefts are deep indentations, sharing the localization of normal slits between the scallops of the posterior MV, but with over 50% the depth

of adjacent scallops.[4] This anomaly is frequently associated with counterclockwise rotation of the papillary muscles, accessory papillary muscle or MV leaflet, and MV prolapse.[5] Our patient presented MR as a consequence of complex MV prolapse with a ruptured chordae, associated with the pseudo-cleft. High LV end-diastolic pressures in the context of the ischemic event and LV systolic dysfunction probably worsened the severity of the MR, as the patient denied any dyspnea prior to hospitalization. Moreover, the question remains whether the rupture of the chordae occurred prior or was related to the ischemic event.

However, even though not entirely responsible for the MR, the presence of the pseudo-cleft has an additional influence on the surgical decision regarding the reparability of the MV. Mantovani et al.[6] showed that 35% of patients with MV prolapse have pseudo-clefts, not seen by 2DE and revealed only by 3DE. The presence of unsolved pseudo-clefts in patients with MV prolapse was associated with poor prognosis after MV repair and a higher recurrence of the MR at follow-up. In this context, MV repair was performed in our patient, and it included the suture of the MV pseudo-cleft.

Conclusions

3D TEE is a useful and feasible technique for correct diagnosis in patients with complex MV disease, especially when etiology is uncertain, and for determining valve repairability. Even though MV pseudo-clefts rarely lead to regurgitation, they are associated with worse postoperative outcomes; therefore, they need to be sutured during MV repair.

Author contributions

Conception and design of the research: Baldea SM, Vinereanu D; Data acquisition and Writing of the manuscript: Baldea SM, Velcea AE; Analysis and interpretation of the data: Baldea SM, Badano LP; Critical revision of the manuscript for intellectual content: Baldea SM, Velcea AE, Badano LP, Vinereanu D.

Potential Conflict of Interest

No potential conflict of interest relevant to this article was reported.

Sources of Funding

There were no external funding sources for this study.

Study Association

This study is not associated with any thesis or dissertation work.

Ethics approval and consent to participate

This study was approved by the Ethics Committee of the Emergency University Hospital Bucharest under the protocol number 15/2.07. All the procedures in this study were in accordance with the 1975 Helsinki Declaration, updated in 2013. Informed consent was obtained from all participants included in the study.

References

1. Lang RM, Mor-Avi V, Sugeng L, Nieman PS, Sahn DJ. Three-dimensional echocardiography: the benefits of the additional dimension. J Am Coll Cardiol. 2006;48(10):2053-69.
2. Amin A, Davis M, Auseon A. Isolated cleft posterior mitral valve leaflet: an uncommon cause of mitral regurgitation. European journal of echocardiography : J Am Soc Echocardiogr. 2009;10(1):173-4.
3. Miglioranza MH, Muraru D, Mihaila S, Haertel JC, Iliceto S, Badano LP. Isolated Anterior Mitral Valve Leaflet Cleft: 3D Transthoracic Echocardiography-Guided Surgical Strategy. Arq Bras Cardiol. 2015;104(5):e49-52.
4. Narang A, Addetia K, Weinert L, Yamat M, Shah AP, Blair JE, et al. Diagnosis of Isolated Cleft Mitral Valve Using Three-Dimensional Echocardiography. J Am Soc Echocardiogr. 2018;31(11):1161-7.
5. McEnany MT, English TA, Ross DN. The congenitally cleft posterior mitral valve leaflet. An anticedent to mitral regurgitation. Ann Thorac Surg. 1973;16(3):281-92.
6. Mantovani F, Clavel MA, Vatury O, Suri RM, Mankad SV, Malouf J, et al. Cleft-like indentations in myxomatous mitral valves by three-dimensional echocardiographic imaging. Heart. 2015;101(14):1111-7.